

RESEARCH ARTICLE

The deubiquitylase USP10 regulates integrin β 1 and β 5 and fibrotic wound healing

Stephanie R. Gillespie, Liana J. Tedesco, Lingyan Wang and Audrey M. Bernstein^{*†}

ABSTRACT

Scarring and fibrotic disease result from the persistence of myofibroblasts characterized by high surface expression of α v integrins and subsequent activation of the transforming growth factor β (TGF β) proteins; however, the mechanism controlling their surface abundance is unknown. Genetic screening revealed that human primary stromal corneal myofibroblasts overexpress a subset of deubiquitylating enzymes (DUBs), which remove ubiquitin from proteins, preventing degradation. Silencing of the DUB USP10 induces a buildup of ubiquitin on integrins β 1 and β 5 in cell lysates, whereas recombinant USP10 removes ubiquitin from these integrin subunits. Correspondingly, the loss and gain of USP10 decreases and increases, respectively, α v/ β 1/ β 5 protein levels, without altering gene expression. Consequently, endogenous TGF β is activated and the fibrotic markers alpha-smooth muscle actin (α -SMA) and cellular fibronectin (FN-EDA) are induced. Blocking either TGF β signaling or cell-surface α v integrins after USP10 overexpression prevents or reduces fibrotic marker expression. Finally, silencing of USP10 in an *ex vivo* cornea organ culture model prevents the induction of fibrotic markers and promotes regenerative healing. This novel mechanism puts DUB expression at the head of a cascade regulating integrin abundance and suggests USP10 as a novel antifibrotic target.

KEY WORDS: Myofibroblast, Integrin, Fibrosis, Scarring, Wound healing

INTRODUCTION

Tissue scarring and fibrotic disease result from the activities and persistence of myofibroblasts that have failed to undergo apoptosis (Abe et al., 2012; Hinz, 2007; Wilson et al., 2007). Myofibroblasts derive from fibroblasts that originate either from resident stromal cells, from fibrocytes (circulating fibroblasts from bone marrow), or from epithelial to mesenchymal transition (EMT), at least in part in response to the transforming growth factor β (TGF β) proteins (Barbosa et al., 2010; He and Dai, 2015; Jester et al., 2002). Contractile myofibroblasts promote wound healing, but if they persist, fibrotic scarring ensues due to overproduction of extracellular matrix, excessive contraction and an autocrine loop of TGF β activity (Van De Water et al., 2013). Integrins promote myofibroblast differentiation by increasing cell adhesion and therefore cellular tension that is required for assembly of alpha-

smooth muscle actin (α -SMA) stress fibers characteristic of myofibroblasts. Integrins also activate latent, matrix-associated endogenous TGF β by binding to the RGD domain in its latency-associated peptide (LAP) (Hinz, 2015; Leask, 2013). An increase in cell-surface expression of α v-containing integrins (α v β 3, α v β 5, α v β 6, α v β 8 and, recently, α v β 1) correlates with fibrosis in many tissues (Henderson and Sheppard, 2013; Leask, 2013; Reed et al., 2015), whereas genetic silencing of α v, and a blocking α v peptide, prevents fibrosis in mice (Henderson et al., 2013; Mamuya et al., 2014), demonstrating that deregulated cell surface expression of α v integrins is critically important to the establishment of fibrotic disease.


We identified the urokinase (uPA, also known as PLAU) pathway as one of the regulators of integrin α v β 5 and myofibroblast differentiation (Bernstein et al., 2007; Wang et al., 2012). Genetic silencing of uPA or uPAR (also known as PLAUR) led to an increase in the cell surface expression of integrin α v β 5 sufficient to drive myofibroblast differentiation (Wang et al., 2012). Correspondingly, uPAR knockout mice have increased collagen content and myofibroblast count, giving rise to dermal scarring, lung and myocardial fibrosis (Kanno et al., 2008; Manetti et al., 2016, 2014). We found that the higher surface expression of α v β 5 stems from a reduced rate of degradation in the endosomal pathway that corresponds with significantly diminished β 5 ubiquitylation (Wang et al., 2012). Furthermore, in primary human corneal fibroblasts (HCFs), it is α v β 5, not α v β 3, that is induced when fibroblasts are converted to myofibroblasts (Wang et al., 2012). Thus, an initial focus on α v β 5 came from these studies in addition to earlier reports that integrin α v β 5 is associated with myofibroblast contraction and activation of localized TGF β (Wipff et al., 2007). In addition, studies in several pathological states, including scleroderma (Asano et al., 2006a,b, 2005), cardiac fibrosis (Sarrazy et al., 2014) and lung fibrosis (Scotton et al., 2009; Zhou et al., 2010), have implicated α v β 5 integrin as a key player in fibrotic-generating outcomes. The role of α v β 1 integrin as a driver of fibrosis has only recently been revealed (Chang et al., 2017; Reed et al., 2015).

Towards the goal of elucidating new pathways that lead to the accumulation of α v integrins on the cell surface, RNAseq was performed (R. Sachidanandam, Icahn School of Medicine at Mount Sinai, NY, unpublished data) on myofibroblasts (induced by uPA silencing) (Wang et al., 2012). Because our previous data suggested that integrin β 5 in these myofibroblasts retained less ubiquitin (Wang et al., 2012), the expression of genes that add ubiquitin (ligases) or remove ubiquitin (deubiquitylases, DUBs) were examined. The RNAseq data revealed that a subset of DUBs were upregulated after uPA silencing. This was confirmed using the g profiler enrichment analysis tool g:GOst (gene group functional profiling) ($P=7.84\times 10^{-3}$) (Reimand et al., 2016). Because cell surface receptors are often degraded through the endosomal pathway, DUBs in our subset that were known to act in this

Icahn School of Medicine at Mount Sinai, Departments of Ophthalmology and Pharmacology and Systems Therapeutics, New York, NY 10029, USA.

^{*}Present address: SUNY Upstate Medical University, Center for Vision Research, Department of Ophthalmology, Syracuse, New York 13210, USA.

[†]Author for correspondence (bernstea@upstate.edu)

 L.J.T., 0000-0001-5927-4469; L.W., 0000-0001-9236-7229; A.M.B., 0000-0002-2537-2594

Received 28 March 2017; Accepted 22 August 2017

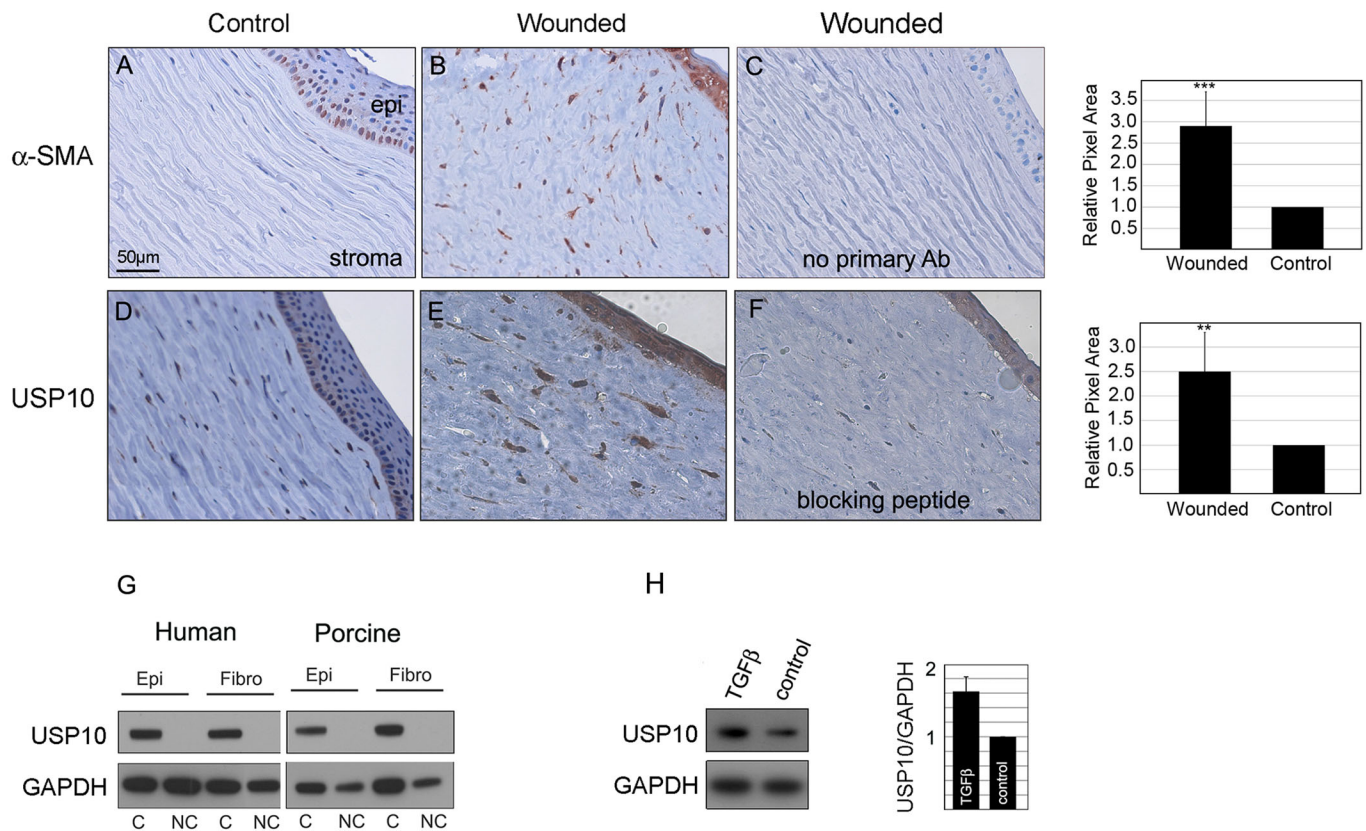


Fig. 1. α -SMA and USP10 are increased in wounded corneas. (A–F) Immunostaining of paraffin-embedded corneal sections comparing control to 2 weeks postwounding. Fibrotic markers are increased in the anterior stroma after wounding: (A,B) α -SMA, 2.9 ± 0.8 -fold increase ($***P < 0.001$); (C) no primary antibody control; (D,E) USP10, 2.5 ± 0.8 -fold increase ($**P < 0.01$); (F) pre-incubation with a USP10 blocking peptide reduced immunostaining. Scale bar: 50 μ m. (G) Western blot of human and porcine primary epithelial cells (Epi) and stromal cells (Fibro) (C, cultured cells; NC, noncultured cells, which are lysed immediately after isolation). (H) HCFs treated with 1 ng/ml TGF β 1 for 24 h induced expression of USP10 ($62 \pm 10\%$ increase). GAPDH was used as a loading control. Data are mean \pm s.d.; $n=3$.

pathway were of particular interest. Secondary screening and biochemical analysis revealed that USP10, which functions in the endosomal pathway (Bomberger et al., 2009, 2010), post-translationally regulates integrin subunits β 1 and β 5, but not β 3. Our data demonstrate a controlling role for USP10 after wounding in determining myofibroblast development and activation of fibrotic TGF β signaling, suggesting that USP10 might be a novel antifibrotic target.

RESULTS

We have used a porcine corneal organ culture model system and human primary corneal stromal fibroblasts to investigate the role of USP10 in wound healing and fibrotic scarring. After stromal wounding or corneal infection, the presence of myofibroblasts and the disorganized newly deposited fibrotic matrix prevents the transmission of light through the cornea (Parapuram and Hodge, 2014). Preventing scarring in the eye is uniquely important since ocular scarring leads to vision loss (Stepp et al., 2014; Whitcher et al., 2001). Unless otherwise noted, all experiments were performed in supplemented-serum free medium (SSFM, see Materials and Methods) without the addition of exogenous growth factors.

USP10 expression is increased after wounding *ex vivo*

We tested whether USP10 expression is upregulated after wounding in an *ex vivo* corneal organ culture model that reproducibly generates a myofibroblast-rich scar. Corneas are wounded by

anterior keratectomy in which a plug of tissue (epithelium, basement membrane and one-third of the anterior stroma) is removed and the corneas are mounted on an agar base and cultured for 2 weeks (Yang et al., 2013). To demonstrate the appearance of myofibroblasts after wounding, tissue was immunostained for the myofibroblast marker α -SMA. In unwounded corneas (control), as expected, there is an absence of myofibroblasts in the stroma (Fig. 1A), while the wounded corneal stroma shows many clearly visible, strongly α -SMA-positive cells (Fig. 1B) (2.9 ± 0.8 -fold increase, $P < 0.001$). In Fig. 1C, the primary antibody was omitted during the staining protocol and, as expected, was negative for α -SMA. Similarly, USP10 protein expression was also upregulated after wounding (Fig. 1D,E). USP10 was increased 2.5 ± 0.8 -fold ($P < 0.01$) in the wounded cornea compared to control. A USP10 blocking peptide profoundly reduced USP10 immunostaining in the stroma and partially in the epithelium, demonstrating the specificity of the anti-human USP10 antibodies to porcine USP10 (Fig. 1F). Of note is that we consistently observed slight and variable nonspecific staining in the basal epithelium of control tissues with all antibodies tested. In addition, although expression of fibrotic proteins in the epithelium is predicted after a penetrating wound (Chandler et al., 2007; Janin-Manificat et al., 2012), all quantification of histological results and conclusions are based solely on the highly specific stromal immunostaining.

We next tested whether a similar upregulation of USP10 expression can be obtained in cells. Culturing cells in serum

induces a wounding phenotype (Kim et al., 2004; Taliana et al., 2005). Human and pig primary corneal epithelial cells and corneal stromal fibroblasts (cultured, C; see Materials and Methods) were compared to cells lysed directly after isolation (uncultured, NC). The data in Fig. 1G demonstrate that in both human and porcine epithelial cell and stromal fibroblasts, USP10 expression is induced in culture cells compared to freshly isolated cells, supporting results obtained in our organ culture model showing that USP10 is induced upon wounding. Finally, we tested whether TGF β , an established, fibrosis-inducing cytokine that is released after wounding, regulates the expression of USP10. Indeed, treating cells with 1 ng/ml TGF β 1 (also known as TGFB1) induced a 62 \pm 10% (mean \pm s.d.) increase in USP10 expression (Fig. 1H).

USP10 regulates integrins β 1 and β 5 post-translationally

Previous studies demonstrate that integrin β 1 and β 5 are ubiquitinated (Wang et al., 2012; Yang et al., 2016), whereas ubiquitylation of integrin β 3 has not been demonstrated. Interestingly, α v does not have the required lysines in the cytoplasmic tail like other α integrin subunits and it is not ubiquitinated (Hsia et al., 2014; Lobert and Stenmark, 2010), suggesting that the β chain of the α v/ β heterodimer triggers degradation. To test the ubiquitylation of β 1, β 3 and β 5 and the role of USP10 in modulating the ubiquitylation state of these integrins, we utilized an ELISA assay that traps ubiquitinated proteins from cell lysates. In this experiment, HCFs were transfected with either USP10 siRNA (consisting of a pool of three targeting siRNAs, see Materials and Methods) or nontargeting siRNA (control siRNA). Lysosomal and proteasomal inhibitors were used to prevent intracellular degradation pathways during USP10 knockdown (leading to accumulation of ubiquitinated proteins) and cells were lysed in the presence of EDTA to promote the dissociation of integrin heterodimers. Ubiquitinated integrins were then detected with anti-integrin antibodies and HRP-linked secondary antibody was quantified by chemiluminescence. Using this assay, we found that β 1 (1.9 \pm 0.4, P <0.05) and β 5 (2.5 \pm 0.9, P <0.05) have significantly more ubiquitin after USP10 silencing (Fig. 2A), whereas β 3 is not significantly affected by USP10 knockdown. Sorting nexin 3 (SNX3) was also tested as a positive control since it is a known substrate of USP10 (Boulikroun et al., 2008). In line with our data on β 1 and β 5, SNX3 has 2.0 \pm 0.5 more ubiquitin after USP10 knockdown (P <0.05). To further probe the effect of USP10 on the ubiquitylation state of the β integrin subunits, we immunoprecipitated integrins β 1, β 3 and β 5, and treated the precipitate with active recombinant USP10 protein. We found that integrins β 1 and β 5 had a reduction in ubiquitylation after treatment with USP10 *in vitro*; integrin β 1 ubiquitylation was reduced by 72 \pm 21% (P <0.05) and integrin β 5 ubiquitylation was reduced by 60 \pm 10% (P <0.01) (Fig. 2B). Again, we observed that USP10 did not significantly affect the ubiquitylation of integrin β 3.

To test whether USP10 regulates the protein levels of α v, β 1 and β 5 integrins, HCFs were transfected with USP10 siRNA, control siRNA (as in Fig. 2A) or scrambled USP10 siRNA (a pool of scrambled USP10 siRNAs based on the pool of targeting USP10 siRNA). Because integrin heterodimers are endocytosed from the cell surface and degraded or recycled together, we would expect that α v protein would be affected along with the β subunits, even if it is not directly targeted by USP10. After treatment with USP10 siRNA, a decrease in USP10 (56 \pm 4%), α v (47 \pm 9%), β 1 (50 \pm 1%) and β 5 (45 \pm 2%) compared to control siRNA was observed (Fig. 2C). There was no significant difference between control siRNA and scrambled USP10 siRNA. Furthermore, USP10 knockdown was repeated using two more unique USP10-targeting siRNAs, demonstrating

similar effects on integrins (Fig. S1). These controls suggest that the decrease in USP10 gene expression and the effect on integrin protein expression is through the specific targeting of USP10. To further test the link between USP10 and integrin protein expression, USP10 was overexpressed in HCFs followed by western blotting for integrin subunits. Western blotting revealed that USP10 overexpression (1.8 \pm 0.2) resulted in an increase in total protein of α v (2.3 \pm 0.7), β 1 (3.9 \pm 1.1) and β 5 (3.3 \pm 0.4) (Fig. 2D). To test for integrin cell surface expression after USP10 overexpression, cell surface biotinylation was utilized. Here, we observed an increase in the fold change of cell surface levels of α v (1.9 \pm 0.4), β 1 (3.0 \pm 1.2) and β 5 (3.1 \pm 0.1) after USP10 overexpression (1.5 \pm 0.1) (Fig. 2E). Although detaching these adherent fibroblasts prior to flow cytometry is challenging and results in reduced cell surface signal, as we previously reported (Wang et al., 2012), using flow cytometry we still observed a trend of increased cell surface expression of integrin α v (1.2 \pm 0.1), integrin β 1 (1.4 \pm 0.04) and integrin α v β 5 (1.6 \pm 0.5) (Fig. S2), supporting the increase in integrin expression by cell surface biotinylation. Interestingly, we consistently observed that small changes in USP10 expression resulted in significant downstream effects.

Although not expected, to test whether USP10 increased integrin proteins levels through an increase in gene transcription, USP10 was overexpressed, and α v, β 1 and β 5 mRNA was quantified using RT-qPCR. We found that α v, β 1 and β 5 RNA expression was not increased when USP10 was overexpressed (2.2 \pm 0.3-fold increase, P <0.05) (Fig. 2F). Finally, we visualized the overlap of integrin α v and vinculin in focal adhesions, and tested whether USP10 overexpression would increase focal adhesion size and number, as such characteristics are markers of the pathological myofibroblast phenotype and increased cell adhesion (Goffin et al., 2006) (Fig. 2G–I). USP10 overexpression increased both the size (3.2 \pm 1.4-fold, P <0.05) and number (1.8 \pm 0.3-fold, P <0.05) of focal adhesions. Together, these data demonstrate that USP10 acts post-translationally on β 1/ β 5 to affect α v, β 1 and β 5 protein levels and α v-containing focal adhesions.

USP10 induces TGF β activity

Integrin heterodimers, which contain the α v subunit, bind to and activate latent TGF β 1 in the extracellular matrix, making them key regulators of TGF β signaling (Henderson and Sheppard, 2013). Because USP10 overexpression generates an increase in cell surface expression of α v β 1/ β 5 integrins, we tested whether it also results in an increase in TGF β activity. To quantify local activation of TGF β , a sensitive co-culture system was utilized (Klingberg et al., 2014; Stuelten et al., 2007; Ulmasov et al., 2016). USP10-overexpressing cells were co-cultured with a SMAD reporter cell line created in an hTERT-human corneal fibroblast cell line (hTERT-HCF) that expresses α v integrins (Jester et al., 2003). In Fig. 3A, we first demonstrate that the hTERT-HCF cell line has low endogenous TGF β activity so that the induction of TGF β activity by USP10 could be easily detected and quantified (Fig. 3A). Next we co-cultured hTERT-HCF USP10 cells or hTERT-HCF control vector cells, each with hTERT-HCF SMAD, for 24 h and quantified luciferase activity in cell lysates. Compared to control cells, USP10-overexpressing cells generated 1.7 \pm 0.3-fold higher luciferase (TGF β activity) (P <0.05) (Fig. 3B). Next, to test whether USP10-mediated TGF β activity is reduced by blocking α v integrins, we incubated α v integrin blocking compound, CHMW12, and control compound, CHMW96 (Henderson et al., 2013), with USP10-overexpressing cells co-cultured with SMAD reporter cells. In this experiment, we

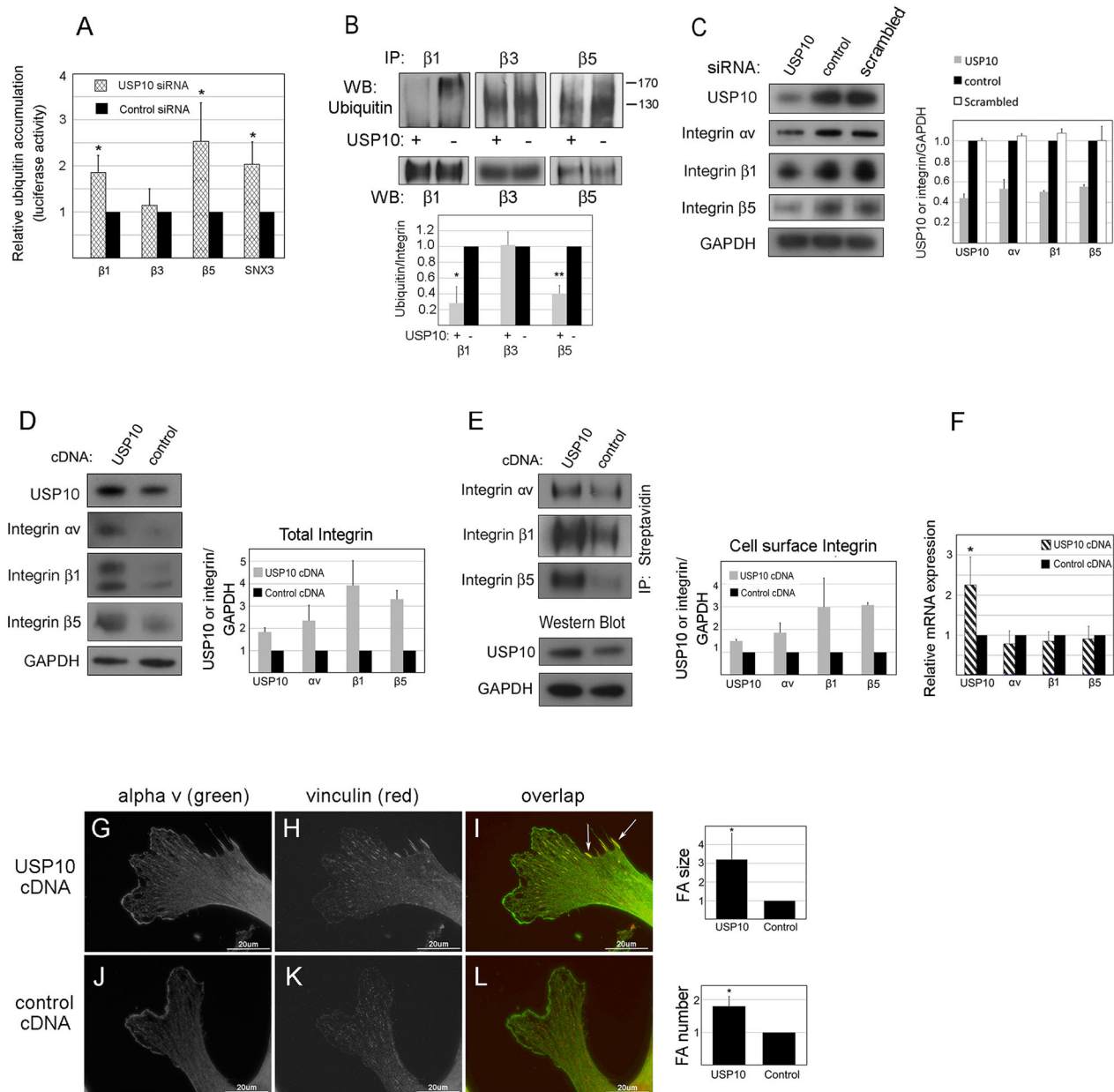


Fig. 2. USP10 removes ubiquitin from integrins $\beta 1$ and $\beta 5$, leading to increased integrin αv , $\beta 1$ and $\beta 5$ total and cell-surface protein levels. (A) HCFs were transfected with USP10 siRNA or control siRNA and cultured in the presence of lysosomal and proteosomal inhibitors. Lysates were incubated in an Ubiquitin S plate (Lifesensors, ubiquitin binding plate) and integrins were detected with antibodies against $\beta 1$, $\beta 3$, $\beta 5$ and SNX3. USP10 siRNA increased ubiquitin on integrins $\beta 1$ (1.9 ± 0.3 -fold, $*P < 0.05$) and $\beta 5$ (2.5 ± 0.9 -fold, $*P < 0.05$) and the control SNX3 (2.0 ± 0.5 -fold, $*P < 0.05$) validating the assay. $\beta 3$ did not increase significantly. Data are mean \pm s.d.; $n = 5$. (B) HCFs were immunoprecipitated with antibodies against integrins $\beta 1$, $\beta 3$ and $\beta 5$ and incubated with active recombinant USP10 protein. USP10 decreased ubiquitylation of integrins $\beta 1$ ($72 \pm 21\%$, $*P < 0.05$) and $\beta 5$ ($60 \pm 10\%$, $**P < 0.01$). USP10 did not affect ubiquitylation of integrin $\beta 3$. The integrin IPs were blotted for integrin $\beta 1$, $\beta 3$ and $\beta 5$ to demonstrate equal loading in each lane. (C) HCFs were transfected with USP10 siRNA, control siRNA, or scrambled USP10 siRNA. Cell lysates were western blotted for USP10, integrins αv , $\beta 1$, $\beta 5$ and GAPDH as a loading control. USP10 siRNA decreased USP10 ($56 \pm 4\%$), αv ($47 \pm 9\%$), $\beta 1$ ($50 \pm 1\%$) and $\beta 5$ ($45 \pm 2\%$). Scrambled USP10 siRNA did not affect USP10 or αv integrin levels when compared to control siRNA. (D) HCFs were transfected with USP10-cDNA or control vector. Cell lysates were western blotted for USP10, integrins αv , $\beta 1$, $\beta 5$ and GAPDH as a loading control. USP10 overexpression increases αv (2.3 ± 0.7 -fold), $\beta 1$ (3.9 ± 1.1 -fold) and $\beta 5$ (3.3 ± 0.4 -fold). (E) Cell-surface biotinylation was used to analyze integrin expression on the cell surface after USP10 overexpression, with an increase in cell surface levels of αv (1.9 ± 0.4 -fold), $\beta 1$ (3.0 ± 1.2 -fold), and $\beta 5$ (3.1 ± 0.1 -fold) observed after USP10 overexpression (1.5 ± 0.1 -fold). GAPDH was used as a loading control. (F) qRT-PCR for USP10, αv , $\beta 1$ and $\beta 5$ after USP10 overexpression compared to control (USP10, 2.2 ± 0.3 -fold increase, $*P < 0.05$; αv , $\beta 1$ and $\beta 5$, nonsignificant). (G–L) HCFs were transfected with USP10 or control cDNA, immunostained for integrin αv (G,J) and vinculin (H,K), and the images were overlapped (I,L). USP10 overexpression increases the size (3.2 ± 1.4 -fold, $*P < 0.05$) and number (1.8 ± 0.3 -fold, $*P < 0.05$) of focal adhesions. Data are mean \pm s.d.; $n = 3$, with 20 cells analyzed per experiment. Scale bars: 20 μ m.

observed a $30 \pm 3.8\%$ decrease in TGF β activity ($P < 0.01$), confirming that αv integrins contribute to TGF β activation in these fibroblasts (Fig. 3C). Because overexpression of USP10 increases active TGF β , and TGF β itself increases TGF β synthesis

(autoinduction) (Kim et al., 1990), we would expect that total TGF β (active and latent) would increase at some level in USP10 cells as well, contributing to the loop of amplified TGF β activity. Indeed, we found a 1.3 ± 0.1 increase in total TGF β from acid-

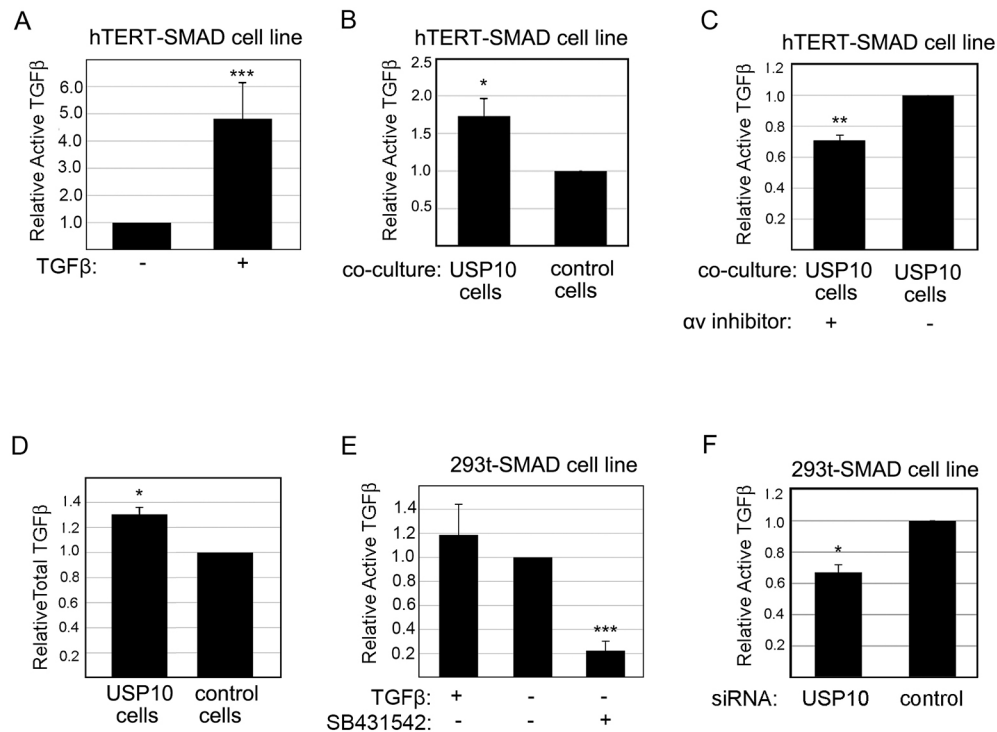


Fig. 3. USP10 expression regulates TGF β activity. (A) hTERT-SMAD reporter cells treated with 1 ng/ml TGF β 1 demonstrated a 4.8 \pm 1.3 increase in response to TGF β (***) (P <0.001). (B) hTERT-SMAD reporter cells were co-cultured with USP10 constitutively overexpressing cells (hTERT-USP10 cells) or control cells (hTERT-vector cells). Co-cultured hTERT-USP10 cells demonstrated 1.7 \pm 0.3-fold higher luciferase activity (P <0.05). (C) hTERT-SMAD reporter cells were co-cultured with hTERT-USP10 cells in the presence of an integrin α v blocking compound (100 nM CWHM12) or control compound (100 nM CWHM96). Blocking α v integrins reduced TGF β activity in cells overexpressing USP10 by 30 \pm 3.8% (** P <0.01). (D) Total TGF β levels were quantified with TGF β ELISA assay of acid-activated cell culture supernatants. USP10-overexpressing cells showed 1.3 \pm 0.1-fold more total TGF β than control cells. (E) 293t-SMAD cells were treated with TGF β , no treatment or TGF β inhibitor. Although TGF β did not significantly increase luciferase expression, the TGF β inhibitor decreased luciferase expression by 78 \pm 7% (***) (P <0.001). (F) 293t-SMAD cells were transiently transfected with USP10 and control siRNA. Cells treated with USP10 siRNA demonstrated a 35 \pm 9% decrease compared to those treated with control siRNA (P <0.05). Data are mean \pm s.d.; n =3.

activated conditioned medium of USP10-cells quantified by TGF β 1 ELISA (P <0.01) (Fig. 3D). Thus, we find that the net increase in active/total (1.7/1.3) TGF β is 33% in USP10 cells compared to control.

To further test the contribution of USP10 to endogenous TGF β activation, we next created another reporter cell line, a HEK-293t SMAD reporter cell line also containing α v integrins (Taherian et al., 2011) that has high endogenous TGF β activity. In Fig. 3E, we demonstrate that the endogenous levels of TGF β are similar to the activity with exogenous TGF β addition, while TGF β inhibitor significantly reduces the signal. Finally, instead of co-culturing, USP10 was silenced directly in these SMAD reporter cells, reducing the TGF β activity by 35 \pm 9% compared to control siRNA (P <0.05) (Fig. 3F). Thus, gain of USP10 increases TGF β signaling, while blocking integrins or reducing USP10 expression reduces TGF β signaling.

USP10 overexpression leads to induction of key fibrotic markers

Since USP10 overexpression increased TGF β activity, we tested whether the consequence of this increase was a rise in other fibrotic markers. The splice variant of fibronectin (FN-EDA) is a key fibrotic marker and like fibronectin (FN) contains the RGD, α v integrin binding domain (Muro et al., 2008; Shinde et al., 2014; White and Muro, 2011). Thus, we tested whether USP10 increases FN-EDA expression in HCFs. HCFs were transfected with USP10 or control cDNA and after 48 h were immunostained for FN-EDA and examined by confocal microscopy. Overexpression of USP10

produced a profound increase (2.7 \pm 0.3-fold compared to control, P <0.01) in FN-EDA (Fig. 4A,B). The organization into deoxycholate (DOC)-insoluble FN reveals that USP10 promotes the cell surface integrin activation required to assemble and organize extracellular FN (Miller et al., 2014). Fractionation of USP10-overexpressing and control HCFs with DOC confirmed the microscopy results demonstrating that FN-EDA protein expression is strongly increased in USP10-overexpressing cells (soluble FN-EDA by 2.0 \pm 0.4-fold and insoluble FN-EDA by 3.8 \pm 0.7-fold) (Fig. 4C). In contrast to the exclusively post-translational effect of USP10 on β 1/ β 5 (Fig. 2), USP10 overexpression of USP10 produced a 4.2 \pm 1.1-fold increase in FN-EDA gene expression (Fig. 4K).

Another central characteristic of the myofibroblast phenotype is α -SMA expression and organization into stress fibers. As demonstrated in the TGF β assay, hTERT cells have very low endogenous TGF β activity, and in the absence of serum, these cells (as well as primary human corneal fibroblasts) will not convert to myofibroblasts unless stimulated. Thus, we compared the morphology of hTERT-HCFs overexpressing USP10 to hTERT-HCF vector control cells and found that 48 h after seeding, 50 \pm 7% of the USP10-overexpressing cells contained organized α -SMA stress fibers (Fig. 4D,F,H) compared to none in control (Fig. 4E,G,I). A similar but less robust result was obtained with transient transfection (data not shown). We also found that α -SMA protein expression was regulated by USP10. Overexpression of USP10 in HCFs increased α -SMA (2.6 \pm 0.4-fold) (Fig. 4J). USP10 also increased α -SMA mRNA modestly (1.4 \pm 0.1-fold) (Fig. 4K).

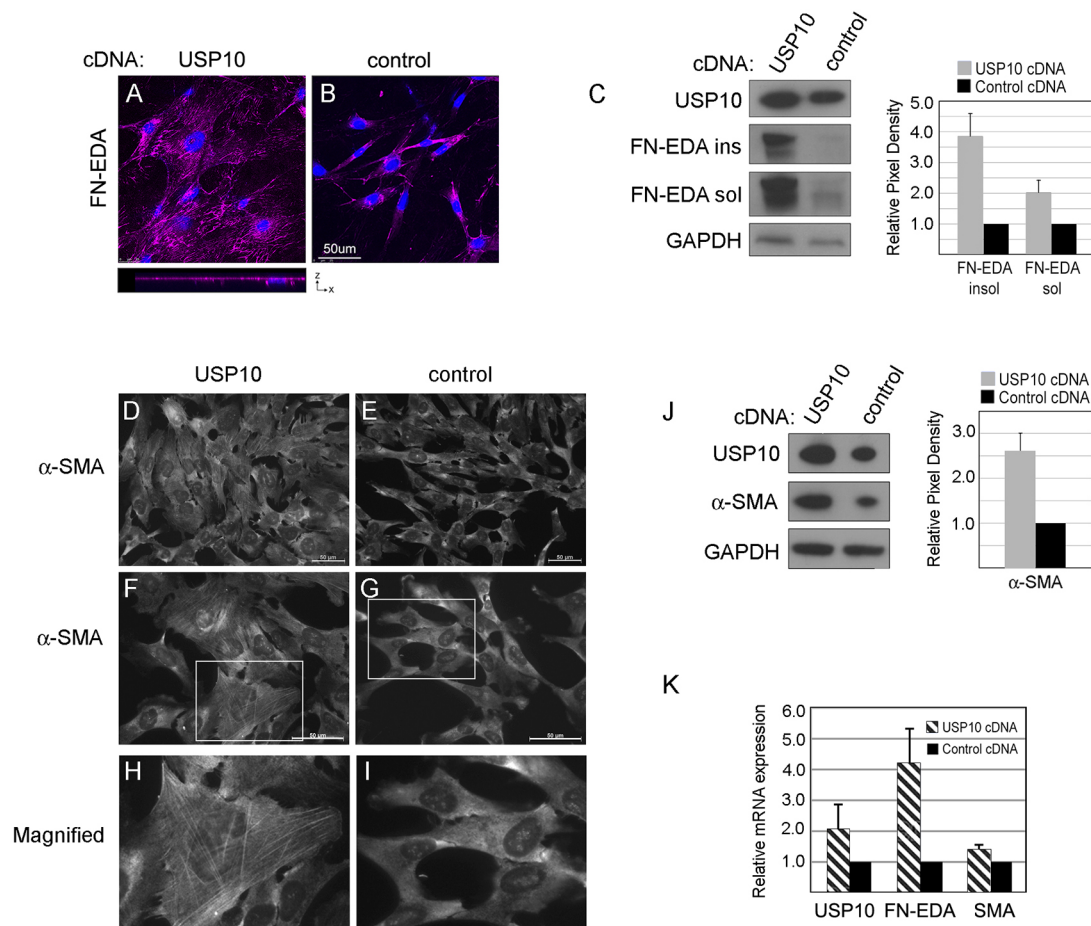


Fig. 4. USP10 regulates the expression and organization of FN-EDA and α -SMA. (A,B) HCFs were transfected with USP10 or control cDNA. Cells were immunostained with antibody against FN-EDA. Images were captured on a Leica laser scanning confocal microscope. Signal was quantified using MetaMorph Analysis software. USP10 overexpression induces a 2.7 ± 0.3 -fold increase in FN-EDA compared to control (** $P < 0.01$). (C) HCFs were transfected with USP10 or control cDNA. Cell lysates were fractionated into DOC-soluble and -insoluble fractions and western blotted for FN-EDA, with GAPDH as a loading control. USP10 cDNA increased soluble FN-EDA by 2.0 ± 0.4 and insoluble FN-EDA by 3.8 ± 0.7 . (D–I) hTERT-USP10 and hTERT-vector cells were immunostained for α -SMA; $50 \pm 7\%$ of USP10-overexpressing cells contained organized α -SMA-containing stress fibers compared to none in control cells. (J) Overexpression of USP10 in HCFs increases α -SMA protein expression by 2.6 ± 0.4 -fold. GAPDH was used as a loading control. (K) USP10 overexpression in HCFs increases the gene expression of α -SMA and FN-EDA: qRT-PCR for USP10 (2.1 ± 0.8 -fold increase), α -SMA (1.4 ± 0.1 -fold increase) and FN-EDA (4.2 ± 1.1 -fold increase). Data are mean \pm s.d.; $n=3$. Scale bars: 50 μ m.

RT-qPCR was also repeated with the hTERT-HCF USP10-overexpressing stable cell line with similar results (data not shown).

Blocking TGF β and α v integrins reduces FN-EDA and α -SMA expression

The above results demonstrate that USP10 increases the key fibrotic markers FN-EDA and α -SMA, likely through the increase in integrin cell-surface expression and subsequent TGF β activation instead of a direct effect on FN-EDA and α -SMA gene transcription. To test this, we incubated primary HCFs overexpressing USP10 with or without the TGF β receptor type I kinase inhibitor, SB431542. We demonstrate by immunocytochemistry (Fig. 5A,B) that the TGF β inhibitor reduced USP10-mediated FN-EDA expression by $82 \pm 0.8\%$ ($P < 0.01$). When tested by western blotting, blocking TGF β reduced FN-EDA protein by $45 \pm 4.7\%$ (soluble) and $70 \pm 3.0\%$ (insoluble) (Fig. 5C). We next expanded these studies to test the effects of blocking TGF β on the organization of α -SMA stress fibers using hTERT-HCF USP10-overexpressing cells. In this case, the TGF β inhibitor totally prevented α -SMA stress fiber formation (Fig. 5D,E). Next, HCFs overexpressing USP10 were treated with CHMW12 or CHMW96 with the α v integrin blocking compound (CHMW12) or

its control (CHMW96). When assayed by immunocytochemistry (Fig. 5F,G), the α v blocking compound reduced FN-EDA by $57 \pm 29\%$ ($P < 0.05$). In western blotting, soluble FN-EDA was reduced by $38.5 \pm 11\%$ and insoluble FN-EDA by $44.3 \pm 10\%$ (Fig. 5H). Similar to blocking TGF β , blocking α v integrins had a dramatic effect on α -SMA stress fiber formation, reducing it from $50 \pm 7\%$ to $5 \pm 3\%$, compared to the control compound, CWHM96, which had no effect ($P < 0.0001$). These data suggest that FN-EDA and α -SMA expression are downstream of USP10 and are regulated, at least in part, by the α v-integrin/TGF β axis. Finally, we asked whether active TGF β will rescue the USP10 knockdown phenotype and, indeed, we found that in cells in which USP10 was knocked down, active TGF β was able to induce myofibroblast differentiation (Fig. 5K,L). These results demonstrate that USP10 deficiency does not produce adherence or mechanosensing defects that would inherently inhibit myofibroblast formation. Furthermore, since active TGF β has a multitude of pleiotropic myofibroblast-inducing effects (Abdalla et al., 2013; Horowitz et al., 2007; Tomasek et al., 2005; Xia et al., 2004), these data also suggest that knockdown of USP10 affects specifically the USP10/ α v pathway and not other potential TGF β -mediated pathways of myofibroblast differentiation.

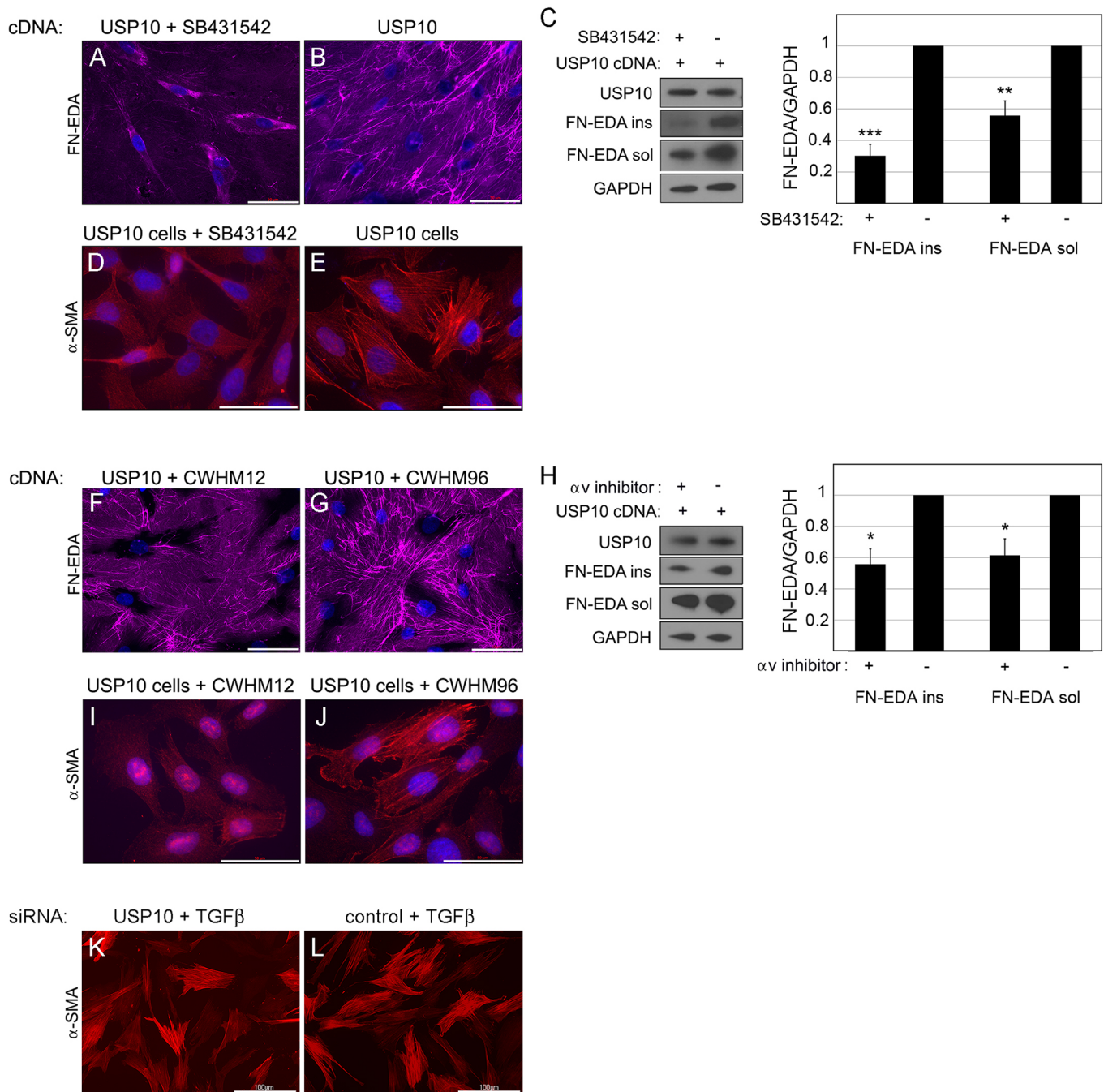


Fig. 5. Blocking TGF β or α v integrins after USP10 overexpression reduces FN-EDA and α -SMA expression. (A,B) HCFs were transfected with USP10 cDNA and cultured in the presence or absence of 10 μ M of the TGF β receptor type I kinase inhibitor (SB431542). Cells were immunostained for FN-EDA. Scale bar: 50 μ m. The TGF β inhibitor reduced FN-EDA expression by 82.3 \pm 0.8% (** P <0.01). (C) The same cells were western blotted for soluble and insoluble FN-EDA. In this assay, blocking TGF β reduced FN-EDA protein by 45 \pm 4.7% (soluble) and 69.7 \pm 3.0% (insoluble). GAPDH was used as a loading control. (D,E) hTERT-USP10-overexpressing cells were treated with or without SB431542 and immunostained for α -SMA. SB431542 prevented α -SMA stress fiber formation. (F,G) HCFs were transfected with USP10 cDNA and cultured in the presence or absence of an α v-integrin blocking compound, 100 nM CWHM12, or nonactive control, CWHM96. Immunocytochemical staining for FN-EDA demonstrated that CWHM12 reduced FN-EDA by 57 \pm 29% (* P <0.05). Scale bar: 50 μ m. (H) Western blotting the α v integrin blocking compound reduced soluble FN-EDA by 39 \pm 10% and insoluble by 44 \pm 9%. GAPDH was used as a loading control. (I,J) CWHM12 reduced α -SMA stress fiber formation from 50 \pm 7% to 5 \pm 3%, whereas the control compound, CWHM96, had no effect. (K,L) HCFs were transfected with USP10 or control siRNA and cultured for 24 h prior to addition of 2 ng/ml TGF β 1 for 48 h and immunostaining for α -SMA. USP10 siRNA did not prevent myofibroblast formation after treatment with exogenous TGF β . Scale bar: 100 μ m. Data are mean \pm s.d.; n =3.

USP10 silencing prevents fibrotic healing

To test whether USP10 silencing decreases fibrosis and improves healing, we targeted USP10 with siRNA after wounding in the porcine *ex vivo* corneal organ culture model (Fig. 1). Because

USP10 is a well-conserved gene, we tested and confirmed that the siRNA, made to human USP10, also targets the porcine USP10 homolog (Fig. 6A). To directly examine the role of USP10 in scarring, the wounded area was treated with one application of

USP10 or control siRNA immediately after wounding. After 2 weeks, the corneas were fixed and analyzed by immunohistochemistry for USP10 and the fibrotic markers α -SMA and FN-EDA. Fig. 6B–J demonstrate that decreasing USP10 by 2.0 ± 0.6 -fold ($P < 0.01$) resulted in a 2.2 ± 0.6 -fold reduction in α -SMA ($P < 0.001$) and a 3.3 ± 1.2 -fold reduction in FN-EDA ($P < 0.01$), as quantified in Fig. 6K.

Qualitatively, we noticed that USP10 knockdown improves cell and matrix alignment in the stroma, which is a critical component of the regenerative healing in the cornea. We found that the number of cells in the wounded corneal stroma (with control siRNA) was 1.7 times greater than in unwounded corneal stroma, as typically expected after wounding (Zieske et al., 2001). However, when comparing unwounded to wounded corneas treated with USP10 siRNA, we found approximately equal cell number, suggesting that reducing USP10 might lead to a reduction in myofibroblast proliferation (Fig. 6L). Importantly, we also found that reduction in the USP10 level was accompanied by regrowth and stratification of the epithelium in a pattern similar to that of control. To test whether USP10 siRNA induced apoptosis of myofibroblasts after wounding, we assayed for apoptosis markers at 1–7 days postwounding; however, we did not observe differences between control siRNA- and USP10 siRNA-treated corneas (data not shown), suggesting that it was myofibroblast formation and the accompanied fibrotic response to wounding that was prevented by USP10 knockdown with siRNA.

Finally, in Fig. 7, using the same model system, we tested whether integrin protein expression is also reduced after treatment with USP10 siRNA. Because there are no antibodies that directly bind to the heterodimer, α v β 1, we separately tested the effect on integrin α v, β 1 and then also on integrin α v β 5. Integrin α v is reduced by $39 \pm 4\%$ ($P < 0.01$), integrin β 1 by $76 \pm 10\%$ ($P < 0.01$) and integrin β 5 by $45 \pm 4\%$ ($P < 0.01$), corresponding with the decrease in fibrotic markers.

DISCUSSION

The α v integrins are important players in the pathways that generate fibrosis. They are expressed on activated pathological myofibroblasts, which secrete fibrotic disorganized ECM and continually activate TGF β , causing scarring and tissue fibrosis (He and Dai, 2015; Hinz and Gabbiani, 2010). Several integrin-targeting therapeutics to treat fibrotic disease are under investigation (Becker et al., 2015; Chang et al., 2017; Kapp et al., 2013; Reed et al., 2015). Regulating integrins through DUB activity might be a novel method of controlling cell-surface integrin expression and resulting pathologies. Recent work has revealed that inhibiting DUBs could be a desirable method of reducing aberrant disease-causing protein accumulation in neurodegenerative diseases and several cancers (Bomberger et al., 2009; Crawford et al., 2011; Deng et al., 2011; Farshi et al., 2015; Hussain et al., 2009; Loch and Strickler, 2012; Riederer et al., 2011).

Here, we report the discovery of USP10 (DUB) as a key regulator of cell surface β 1 and β 5 integrin expression. We show that USP10 protein levels increase after wounding both in an *ex vivo* model of wounding and in cell culture (Fig. 1), and that this increase is accompanied by accumulation of integrins β 1 and α v β 5, induction of TGF β activity, expression of key fibrotic markers FN-EDA and α -SMA, and increased focal adhesion size (Figs 2–4). Blocking α v integrins or TGF β signaling after USP10 overexpression reduced or eliminated USP10-mediated myofibroblast differentiation, FN-EDA and α -SMA protein expression and integrin-mediated organization of FN-EDA fibrils and α -SMA stress fibers (Fig. 5).

Studies on myofibroblasts and surrounding ECM have reported that myofibroblasts specifically activate TGF β through matrix contraction, and that decellularized ECM from myofibroblasts contains increased active TGF β compared to fibroblast ECM (Klingberg et al., 2014; Wipff et al., 2007). Our data suggest that a combination of USP10-induced cell surface integrin accumulation, increase in total TGF β and, perhaps, myofibroblast-ECM contribute to an increase in local TGF β activity that drives a dramatic phenotypic shift from fibroblast to myofibroblast and perpetuates a cycle of TGF β auto-activation and myofibroblast persistence. Our finding that myofibroblasts are still generated after USP10 knockdown and in the presence of exogenous TGF β suggest that USP10-deficient cells are mechanically still able to respond to the TGF β stimulus, and supports our conclusion that USP10 induces TGF β through the integrin α v axis. Our *ex vivo* organ culture data (Figs 6 and 7) suggest that modulating integrins by DUBs might be a powerful method to regulate cell phenotype and perhaps pathological outcomes.

We previously found that integrin α v β 5 is degraded in the endosomal pathway but in myofibroblasts, β 5 has significantly reduced ubiquitylation and degradation with increased cell surface α v β 5 protein expression (Wang et al., 2012). In searching for the mechanism responsible for the surface accumulation of integrin we examined the effect USP10 regulation has on integrin ubiquitylation. Ubiquitylation occurs on lysine residues of the cytoplasmic tail of the integrin. The cytoplasmic tails of integrins β 3 and β 5 each contain four lysines, and integrin β 1 contains six (Fig. S3) (Liu et al., 1996; Pasqualini and Hemler, 1994). Integrin α v has only one lysine, located in a conserved consensus sequence (GFFKR) that is important for integrin heterodimer stability (Lobert and Stenmark, 2010). This sequence is located just below the transmembrane region and is not ubiquitylated (Hsia et al., 2014). Thus, we focused on the ubiquitylation of stromal cell β integrins (β 1/ β 3/ β 5) (Masur et al., 1993; Wang et al., 2012).

Here, we determined that knocking down USP10 resulted in an increase in β 1 and β 5 ubiquitylation but not β 3 (Fig. 2A), and that USP10 is able to remove ubiquitin from both β 1 and β 5 subunits, *in vitro* (Fig. 2B). The change in α v protein levels we observed with loss and gain of USP10 is indirect, owing to retention of the β 1 and β 5 partner (less DUB, more ubiquitylation and more degradation of the heterodimer, or more DUB, less ubiquitylation and less degradation of the heterodimer).

A previous study demonstrated that α 5 β 1 binding to FN was necessary for ubiquitylation of α 5 and degradation of the internalized FN/ α 5 β 1 complex in the endosomal pathway. Furthermore, that degradation was necessary for cell migration (Lobert et al., 2010). The authors proposed that reduced degradation of integrins would favor the recycling of the ECM bound integrin to the cell surface, where the complex would form dysfunctional adhesion sites, yielding pathological cell adhesion and a buildup of ECM. Our data not only fit this hypothesis but also, importantly, advance the understanding of the mechanisms that drive pathological myofibroblast persistence. It remains to be determined what other integrin heterodimers are regulated by which DUBs and how specificity is conferred. Since we found that β 1 was regulated by USP10, we would predict that other α / β 1 heterodimers such as α 5 β 1 are affected by USP10. For instance, although the USP10-mediated increase in FN-EDA gene and protein expression (Fig. 4) was likely caused by enhanced TGF β activity, the increase in DOC-insoluble FN is produced from integrin-mediated organization of FN (Wierzbicka-Patynowski and Schwarzbauer, 2003), suggesting that α 5 β 1 integrin expression and/or activity is augmented directly by USP10. Alternatively, like we

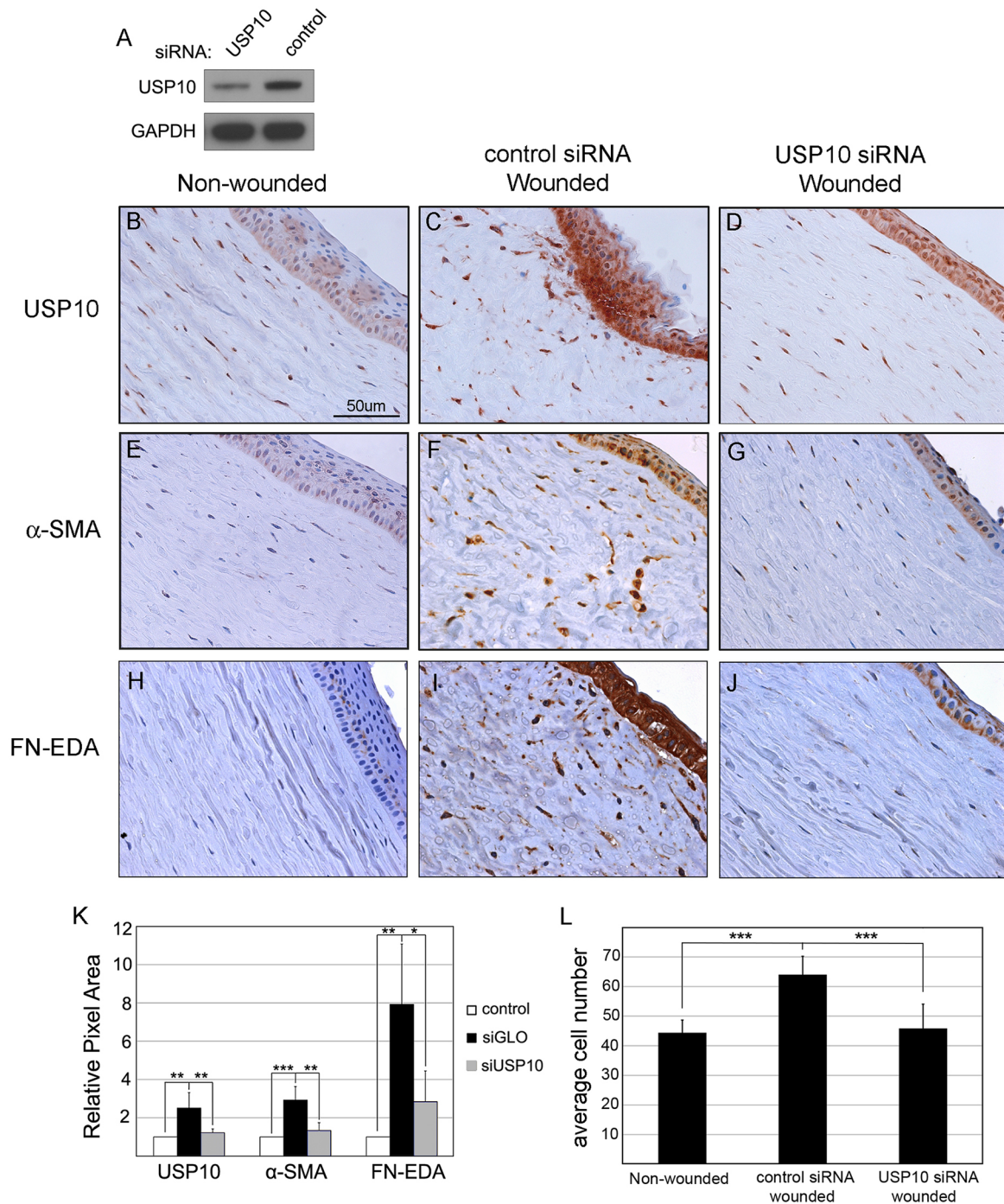


Fig. 6. Silencing USP10 *ex vivo* decreases the fibrotic wound healing response. (A) Primary porcine corneal fibroblasts were transfected with human USP10 or control siRNA and western blotted for USP10, with GAPDH as a loading control. (B–J) Porcine corneas were cultured as in Fig. 1 and either unwounded (control) or wounded and treated with control or USP10 siRNA. (B–M) After treatment with USP10 siRNA, USP10 was reduced 2.0 ± 0.6 -fold ($**P < 0.01$), α -SMA 2.2 ± 0.6 -fold ($***P < 0.001$) and FN-EDA 3.3 ± 1.2 -fold ($**P < 0.01$). Immunostaining of wounded corneas treated with USP10 siRNA were equal to nonwounded controls in all experiments; the differences between control and USP10 knockdown were nonsignificant. (The increase in FN-EDA between control and wounded was not described in Fig. 1; thus, here we report that FN-EDA was increased 7.3 ± 2.7 -fold after wounding, $**P < 0.01$.) Scale bar: 50 μ m. Data are mean \pm s.d.; $n = 3$. Statistical significance was determined by one-way ANOVA with Bonferroni's test. (K) Quantification of USP10, α -SMA and FN-EDA after treatment with USP10 siRNA. (L) Corneal wounding increased average stromal cell number from 44 ± 4 (nonwounded) to 64 ± 6 (control siRNA, wounded) ($***P < 0.001$). Silencing USP10 decreased average cell number from 64 ± 6 (control siRNA, wounded) to 45 ± 8 (USP10 siRNA, wounded) ($***P < 0.001$). There was no significant difference between the number of cells in nonwounded compared to USP10 siRNA wounded conditions.

and others have demonstrated, $\alpha 5\beta 1$ activity might be affected through crosstalk with αv integrins (Defilles et al., 2009; Wang et al., 2012). Addressing this question directly, a recent study

demonstrated that αv integrins bind first to FN, recruiting $\alpha 5\beta 1$ to adhesion sites and that integrin crosstalk induced $\alpha 5\beta 1$ integrin clustering and downstream signaling to strengthen adhesion

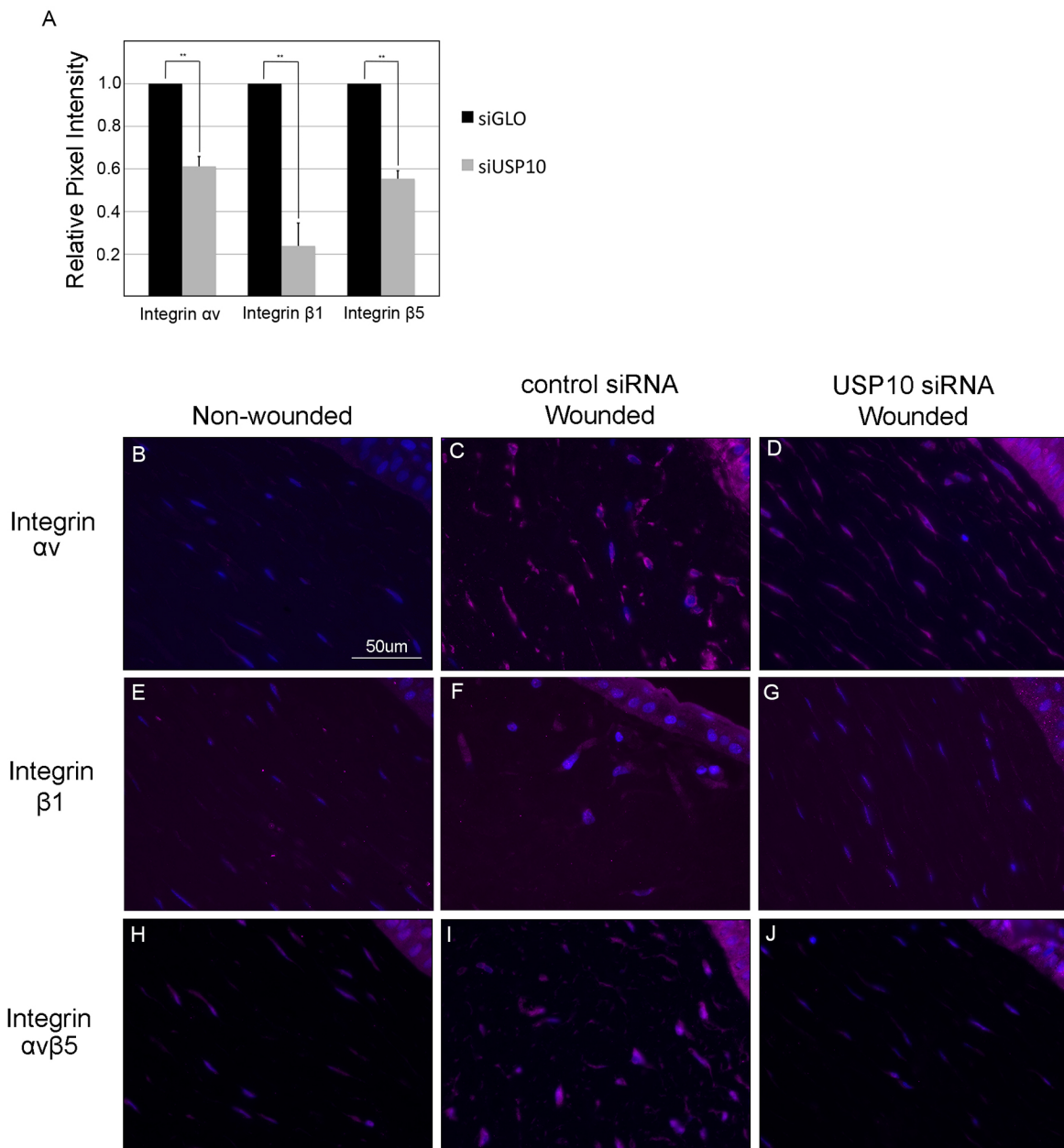


Fig. 7. Silencing USP10 *ex vivo* decreases integrins αv , $\beta 1$ and $\beta 5$. (A) Quantification of integrins αv , $\beta 1$ and $\beta 5$ after treatment with USP10 siRNA compared to control siRNA. Threshold intensity levels were too high to detect nonwounded control staining. (B–D) Compared to control siRNA, integrin αv was reduced by 39 \pm 4% (** P <0.01). (E–G) Integrin $\beta 1$ was decreased by 76 \pm 10% (** P <0.01) after treatment with USP10 siRNA. (H–J) Compared to control siRNA, integrin $\beta 5$ was decreased by 45 \pm 4% (** P <0.01) after treatment with USP10 siRNA. Scale bar: 50 μm . Data are mean \pm s.d.; n =3.

(Bharadwaj et al., 2017). Thus, it seems likely that USP10 could affect $\beta 1$ integrin either directly or indirectly through αv integrin crosstalk.

There is only a limited context in which to compare our results on myofibroblasts, integrins and DUBs. In terms of DUBs and myofibroblasts, a recent study demonstrated that the DUB UCHL1 is significantly induced during stellate cell activation, and knockdown of UCHL1 blocks progression of CCl₄-induced fibrosis in mice (Wilson et al., 2015). In terms of DUBs and integrins, one group demonstrated that the DUB ataxin-3 regulates integrin $\alpha 5$ and the dysregulation of $\alpha 5$ by ataxin-3 is a critical component of the neurological disorder Machado–Joseph disease (do Carmo Costa et al., 2010). USP10 is also a DUB for several nonintegrin proteins and thus USP10 regulation is likely to be

tissue- and context-specific. The new USP10 role we describe aligns with its regulation of other cell surface receptors in different cell types. For example, USP10 gene silencing increases the ubiquitylation and lysosomal degradation of the cystic fibrosis transmembrane conductance regulator (CFTR) in airway epithelial cells, whereas overexpression leads to cell surface accumulation of CFTR (Bomberger et al., 2009, 2010). In addition, USP10 was found to have an indirect effect on the amiloride-sensitive epithelial Na⁺ channel (ENaC) in HEK-293 cells. In this case, USP10-mediated stabilization of the nexin protein, SNX3, indirectly induced the cell surface accumulation of ENaC (Boukroun et al., 2008).

USP10 is also a DUB for p53 (also known as Tp53) (Yuan et al., 2010). Under certain conditions, USP10 is phosphorylated and

translocated to the nucleus, where it deubiquitylates p53, stabilizing p53 protein levels (Yuan et al., 2010). USP10-mediated action on p53 might be important in wound healing. Temporary knockdown of p53 has been utilized as a pharmacological method to improve healing after kidney organ transplant and kidney injury (Imamura et al., 2010; Molitoris et al., 2009; Thompson et al., 2012). Thus, along with the effects on integrins, a USP10-mediated temporary reduction in p53 might also aid in regenerative healing. Finally, USP10 activity is also increased under conditions of increased inflammation (Pan et al., 2014) and in the presence of environmental toxins, where it is localized to stress granules to combat ROS activity (Takahashi et al., 2012). Although it is unclear how these seemingly diverse functions are interconnected, a unifying theme for USP10 appears to be its induction by cellular stress. Based on our data, we propose that while anti-stress mechanisms rescue cells from death (Horowitz et al., 2007), the byproduct of the USP10-induced prosurvival mechanisms in fibroblasts is myofibroblast persistence and subsequent fibrotic scarring.

Our initial result derived from the finding that uPA/uPAR knockdown lead to an increase in cell surface $\alpha\beta 5$ integrin (Wang et al., 2012) and here we show that this is due at least in part to an increase in the gene expression of USP10. Although the link between uPA/uPAR and USP10 gene expression is presently unknown, since a uPAR knockout mouse model displays a high myofibroblast count, dermal scarring, lung and myocardial fibrosis (Kanno et al., 2008; Manetti et al., 2016, 2014), and we found that a disruption of uPA/uPAR cell surface binding (Bernstein et al., 2007) and uPA/uPAR knockdown in primary human cells induces myofibroblast differentiation (Wang et al., 2012), perhaps continued exploitation uPA/uPAR knockout model systems would further elucidate drivers of fibrotic disease. Furthermore, although promising new therapies for fibrosis target integrins extracellularly (Conroy et al., 2016), preventing scarring (acute wound) versus fibrosis (chronic condition) might require different approaches. Blocking integrins directly after wounding has been shown to prevent re-epithelialization and, therefore, ultimately prevent healing (Duperret et al., 2016 and our observations), whereas reducing, but not directly blocking, cell-surface expression of integrins after wounding could prevent the induction of scarring pathways and promote regenerative healing.

In summary, our discovery is the first to connect a DUB to integrin-mediated myofibroblast differentiation. We show that wounding induces upregulation of USP10. Our working model is that USP10, by removing ubiquitin from the integrin $\beta 1$ and $\beta 5$ subunits, protects them from degradation in the endosomal/lysosomal pathway promoting their recycling and accumulation on the cell surface. This initiates a sequence of integrin-mediated TGF β activation, myofibroblast development, excessive matrix formation, and an autocrine loop of local TGF β activation, promoting further USP10 expression. This cycle would keep the forward feed loop going, contributing to myofibroblast persistence and scarring (Fig. 8). Because our results strongly implicate USP10 as a gatekeeper for regulation of surface expression of $\alpha\beta$ integrins and fibrotic scarring, we propose that targeting and reducing USP10 levels will redirect cells into a regenerative healing pathway.

MATERIALS AND METHODS

Cell culture

Human cadaver corneas from unidentifiable diseased subjects were obtained from The National Disease Research Interchange (NDRI, Pittsburgh, PA). The Icahn School of Medicine Institutional Review Board has informed us that, as described under Title 45 CFR Part 46 of the Code of Federal

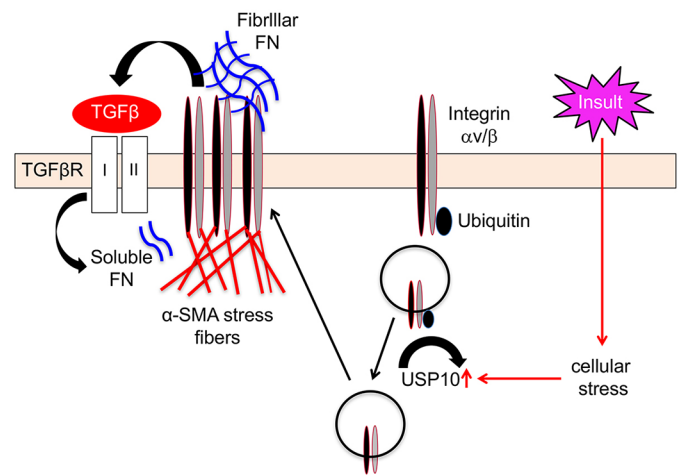


Fig. 8. Working model for the USP10-mediated induction of a pathological myofibroblast. Acute and chronic injury to tissues induces cellular stress pathways. Our working model is that tissue wounding and fibrotic growth factor activity induces an increase in USP10 protein expression and DUB activity. USP10 removes ubiquitin from internalized $\alpha\beta 1/\beta 5$ integrins, saving them from degradation and promoting integrin recycling. The increase in USP10 DUB activity shifts the balance of integrin degradation/recycling to yield a net accumulation of integrin on the cell surface. This in turn leads to pathological cell adhesion, activation of TGF β signaling, and the organization of α -SMA containing stress fibers.

Regulations, unidentifiable cadaver tissue does not constitute research in human subjects. Hence, the experiments performed in this report do not require their approval or waiver. HCFs were derived from the stroma of human corneas obtained from NDRI. HCFs were isolated as described previously (Bernstein et al., 2007) and maintained in complete media (DMEM-F12, Invitrogen) with 10% FBS (Atlanta Biologicals) with ABAM and Gentamicin (Invitrogen). For experiments, except where noted, cells were plated on 10 μ g/ml bovine collagen (Purcol, Advanced Biomatrix) in SSFM [DMEM-F12 plus RPMI-1640 Vitamin Mix, ITS liquid media supplement, 1 mg/ml glutathione (Sigma-Aldrich), 2 mM L-glutamine, 1 mM sodium pyruvate, 0.1 mM nonessential amino acids (Invitrogen) with ABAM and Gentamicin].

Cell lines were created using standard lentiviral infection technique: SMAD-luciferase/GFP reporter (pGreenFire Lenti-Reporter, System Biosciences) with immortalized hTERT-HCFs [a gift from Dr James Jester, UC Irvine School of Medicine, Irvine, CA (Jester et al., 2003); hTERT-SMAD]; SMAD-luciferase/GFP reporter with HEK-293t [293T/17 (HEK 293T/17) (CRL-11268, ATCC); 293t-SMAD]; USP10-overexpressing immortalized hTERT-HCFs (hTERT-USP10); empty vector overexpressing immortalized hTERT-HCFs (hTERT-vector). Selection was by puromycin (hTERT-SMAD, 293t-SMAD, hTERT-USP10, hTERT-vector). All cells were routinely tested for contamination including mycoplasma.

Organ culture

Whole porcine eyes were obtained from Pel-Freez (Rogers, AR). Lids were removed from globes and eyes were submerged in 10% iodine and then rinsed thoroughly with PBS. A 6 mm trephine was used to wound the anterior cornea including the epithelium, basement membrane and anterior stroma and the excised tissue was removed with a surgical blade. Wounded and control (nonwounded) corneas were mounted on a mix of 1% agar, 1 mg/ml bovine collagen in DMEM-F12, and cultured for 2 weeks in SSFM plus 1 mM Vitamin C (2-0-aD Glucopyranosyl-Ascorbic Acid, Wako). Gene knockdown was performed by treating cells with USP10 siRNA or siGLO siRNA with Lipofectamine 2000 (Invitrogen) according to the standard protocol. After 3 h, the siRNA was washed out of the wound bed with SSFM plus Vitamin C. After a 2 week incubation, during which the medium was changed every 48 h, tissue was fixed in 10% formalin and sections were generated at the Histology-Biorepository Shared Resource Facility at Icahn School of Medicine at Mount Sinai. Five slices from each

cornea in each experiment were analyzed. Using ImageJ, threshold pixel intensity was set for all images. The area greater than the threshold measurement in the corneal stroma was quantified for each image. All results are reported as mean±s.d.

Antibodies and reagents

Integrin $\beta 5$ antibody for flow cytometry (2.5 $\mu\text{g}/10^6$ cells), and immunoprecipitation (IP) (10 $\mu\text{g}/\text{ml}$) was from R&D Systems (MAB2528); integrin $\beta 5$ antibody for western blotting (1:300) and immunoprecipitation (IHC) (1:100) was from Abcam (ab15459). USP10 (for western blotting, 8501; 1:1000), αv (4711; 1:300), $\beta 1$ (9699; 1:1000) and GAPDH (2118; 1:3000) antibodies were from Cell Signaling. Flow cytometry antibodies for $\beta 1$ (MAB17781) and αv (MAB12191) (both used at 2.5 $\mu\text{g}/10^6$ cells) were from R&D Systems. Immunoprecipitation antibodies for $\beta 1$ (MAB2528) and $\beta 3$ (MAB3050) (both used at 10 $\mu\text{g}/\text{ml}$) were from R&D systems. FN-EDA [for immunocytochemistry (ICC), 1:200; for western blotting, 1:1000; for histology, 1:200] (F6140) and α -SMA (for ICC, 1:200; for histology, 1:200) (C6198) were from Sigma. USP10 antibody for histology was from Bethyl Laboratories (A300-900A; 2 mg/ml). Ubiquitin antibody (P4D1; 1:1000) was from Cell Signaling. Secondary Alexa-Fluor-647-conjugated antibodies were from Molecular Probes (1:400), and all HRP-conjugated secondary antibodies were from Jackson Laboratories (1:3000). Active recombinant USP10 protein was from Lifesensors. Streptavidin beads were from Pierce and Protein G Dynabeads were from Invitrogen. The nontargeting fluorescent nucleotide control (siGLO) was from Dharmacon. USP10 siRNA was a pool of three siRNAs (5'-GAAGUUCAUCCUCUGUAU, 5'-AUACAGAGGAAUGAACUUC-3'; 5'-GAGGAAAUGUUGAACCUAA-3', 5'-UUAGGUUC-AACAUUUCCUC-3'; 5'-CCAGUCUCAUUGCUUAGUA-3', 5'-UACUAAGCAAUGAGACUGG-3') from Santa Cruz Biotechnology (sc-76811). USP10 scrambled siRNA was a pool of three siRNAs from Thermo Fisher Scientific (5'-GUCACAUCUAUCGUUAGUU-3', 5'-AACUAAC-GAUAGAUGUGAC-3'; 5'-GACAGGUAGACGAAUUAU-3', 5'-AU-AUAUUCGUCUACCUGUC; 5'-GCUUCAUGCUUCGAAUACU-3', 5'-AGUAUUCGAAGCAUGAAG-3'). For additional USP10 siRNA control experiments, HCFs were transfected with two USP10 siRNAs (Dharmacon) that target unique USP10 sequences from the pool of USP10 siRNAs (5'-UGAGUUUGGUGUGCAUGAA-3' and 5'-GAUAAAAUCGUGAGGG-AUA-3').

USP10 cDNA (Flag-HA-USP10; 22543) for transient overexpression was from Addgene [deposited by Wade Harper (Sowa et al., 2009)]. Lentiviral cDNA USP10 (pLenti-GIII-CMV-hUSP10-Cterm-HA) and Vector (pLenti-III-Blank Control Vector) were from ABM Applied Biological Material. SMAD luciferase/GFP reporter (pGFP-SMAD reporter cDNA; TR203PA-P) was from System Biosciences. TGF β blocking compound SB431542 was from Tocris. Integrin αv blocking compound (CWHM12) and control (CWHM96) were a generous gift from Dr David Griggs, Saint Louis University, St. Louis, MO.

Western blots

Cells were lysed in RIPA buffer (0.1% SDS, 0.05 M Tris, 0.15 M NaCl, 0.5% Na Deoxycholate, 1% Triton) plus complete protease inhibitor tablet (Roche) and PMSF (Thermo Fisher Scientific). Then, 15 mg protein was separated on 10% NuPAGE gels under reducing conditions (except when blotting for integrin $\beta 3$, which is run under nonreducing conditions) and transferred to PVDF membranes. Primary antibody was added to 5% BSA in TBST and secondary antibody was added to 1% milk in TBST. Bands were visualized using CL-XPosure Film (Thermo Fisher Scientific). Fibronectin DOC soluble and insoluble western blots were performed using the protocol previously described by Sechler et al. (1996).

Cultured and noncultured epithelial and stromal cells

For corneal epithelial cell culture, human corneas were cut into quarters and incubated overnight in bicarbonate-free DMEM/F12 with 5 mg/ml Dispase II (Roche) at 4°C under slow (>60 rpm) tilting motion. The spontaneously separated epithelial sheets were dissociated into single cells by trypsinization (15 min). The pelleted cells were resuspended in Cnt-PR (Cell-N-Tech) and seeded in six-well plates at 4000 cell/cm². After 2 days in

culture, the cells were lysed in RIPA buffer plus protease inhibitors. For noncultured epithelial cell analysis, the cells were pelleted and resuspended in RIPA buffer plus protease inhibitors directly after isolation.

For corneal stromal cell culture, human corneas were cut into quarters and incubated overnight in bicarbonate-free DMEM/F12 with 5 mg/ml Dispase II (Roche) at 4°C under slow (>60 rpm) tilting motion. The corneal stromas were then incubated for 3 h at 37°C with shaking in collagenase in bicarbonate-free DMEM/F12. The isolated stromal cells were pelleted and resuspended in RIPA plus protease inhibitors (noncultured cells) or in complete media and cultured for 2 days prior to lysing (cultured cells).

Transient transfections

Transient transfection was performed using the Amaxa Nucleofection system and Lonza P3 reagent. HCFs were transfected using 10 μM USP10 siRNA, control siRNA (siGLO), scrambled USP10 siRNA, 1.5 ng USP10 cDNA or control cDNA, and seeded on collagen in SSFM without antibiotics. Cells were analyzed after 24–48 h. Knockdown/overexpression was confirmed by western blotting and RT-qPCR.

Ubiquitin S assay

HCFs were transfected with USP10 siRNA or siGLO and seeded in 1% FBS. After 8 h, 5 μM MG132 and 10 μM chloroquine (Enzo Life Sciences) was added to inhibit lysosomal and proteasomal degradation. After 16 h, cells were lysed in RIPA with protease inhibitors, phosphatase inhibitor (HALT), and DUB inhibitors (NEM and PR619). After determining protein concentration, lysate was added to Ubiquitin S plates (Lifesensors) at a concentration of 400 $\mu\text{g}/\text{ml}$. Primary antibodies against αv (R12-2222), $\beta 1$ (R12-2927), $\beta 3$ (B7118), $\beta 5$ (C0235), and SNX3 (C18897) were from Assay Biotech. Ubiquitin S anti-rabbit secondary and detection reagent (Lifesensors) were used. Luciferase expression was read by a Biotek plate reader.

Immunoprecipitation and immunoblotting for ubiquitin

Cells were treated with 5 μM MG132 and 10 μM chloroquine for 3–4 h prior to lysing. Cells were lysed in RIPA buffer (0.1% SDS, 0.05 M Tris, 0.15 M NaCl, 0.5% sodium deoxycholate, 1% Triton) plus complete protease inhibitor tablet (Roche), PMSF (Thermo Fisher Scientific), NEM (Pierce) and PR-619 (Lifesensors). Lysate was incubated overnight with antibodies against αv (Abcam), and $\beta 1$, $\beta 3$ and $\beta 5$ (R&D Biosystems). The following day, protein G Dynabeads (Invitrogen) were added for 1 h at 4°C. After incubation of beads with lysate, active recombinant USP10 (Lifesensors) was added to the beads in 50 mM HEPES (pH 7.5), 100 mM NaCl, 5% glycerol, 5 mM MgCl₂, 1 mM ATP and 1 mM DTT buffer (Dupont et al., 2009) and incubated for 30 min at 30°C. Precipitate was separated on 4–12% NuPAGE gels under reducing conditions and transferred to PVDF membranes. The membrane was treated with denaturing solution (Sigismund and Polo, 2016) for 30 min at 4°C prior to incubating with P4D1 ubiquitin antibody (Cell Signaling Technology). The membranes were blotted for integrin $\beta 1$, $\beta 3$ and $\beta 5$ to demonstrate equal loading in each lane.

Cell surface biotinylation

5 ml of 0.5 mg/ml EZ-Lnk Sulfo-NHS-LC-Biotin was added to HCFs transfected with USP10 cDNA or vector cDNA for 30 min at room temperature. Cells were quenched with 100 mM Tris for 10 min at room temperature, then lysed with RIPA plus complete protease inhibitor tablet and PMSF. Lysates were incubated overnight with streptavidin magnetic beads (Pierce). Beads were washed with TBS with 0.1% Tween and incubated for 5 min at 100°C with 4× SDS PAGE loading buffer and 20% betamercaptoethanol. The supernatant was separated on a 10% NuPAGE gel under reducing conditions and transferred to PVDF membranes. Primary antibodies against integrin αv , $\beta 1$ and $\beta 5$ were added to 5% BSA in TBST and secondary antibody was added to 1% milk in TBST. Bands were visualized using CL-XPosure Film (Thermo Fisher Scientific).

Flow cytometry

Cells were detached with Cell-Dissociation Solution, non-enzymatic (Sigma-Aldrich) with 0.05% sodium azide at 37°C and centrifuged. Cells

were incubated with 2.5 µg/ml primary antibody and Alexa Fluor 488-conjugated secondary antibody at 4°C. After washing, cells were stained with PI α and analyzed in a flow cytometer (Accuri c6).

ICC

Cells were fixed with 3% paraformaldehyde (Fisher Scientific, Fair Lawn, NJ), permeabilized with 0.1% Triton X-100 (Sigma-Aldrich), and blocked with 3% normal mouse serum (Jackson ImmunoResearch). Cells were incubated in primary antibody against vinculin, integrin α v, SMA-cy3 or FN-EDA. Cy5-conjugated goat-anti-mouse IgM was used as a secondary to FN-EDA. α -SMA, vinculin, integrin coverslips were viewed with a Zeiss Axioskop microscope and images were captured using a Zeiss Axioplan2 microscope with a SPOT-2 CCD camera (Diagnostic Instruments). FN-EDA stained coverslips were imaged using a Leica SP5 confocal microscope, and signal was quantified by Metamorph software. α v integrins were blocked with 100 nM CWHM12 (described by Sheppard et al., 2013). Control compound was 100 nM CWHM96, the inactive R-enantiomer of CWHM12. TGF β signaling was inhibited with 10 µM SB431542 (Tocris), a TGF β receptor type I kinase inhibitor. For the rescue experiment, HCFs were transfected with USP10 or control siRNA and cultured for 24 h to allow for gene knockdown prior to addition of 2 ng/ml TGF β 1 for 48 h. Immunostaining was for α -SMA.

Immunohistochemistry

Slides were deparaffinized using SafeClear (Protocol, Fisher Healthcare) for 10 min two times, then transferred into 100% EtOH, 70% EtOH, 50% EtOH and ddH₂O for 5 min each. Slides were then microwaved two times at 50% power for 5 min in citrate buffer for antigen retrieval. After cooling, slides were washed in PBS and placed in 1% Triton in PBS for cleaning. Tissue was blocked with 3% normal goat serum in PBS for 1 h, and then treated with primary antibody overnight. After washing in 0.1% Tween PBS, slides were placed in 3% H₂O₂ for 10 min to block endogenous peroxidase. Tissue was then incubated with HRP secondary antibody (1:200) for 1 h. After washing in 0.1% Tween PBS, tissue was treated with DAB (Vector Laboratories). Tissue was counterstained in Harris Modified Hematoxylin (Fisher Chemical) and stained with Scott's Bluing Reagent (Ricca Chemical Company), before dipping in ddH₂O, 50% EtOH, 70% EtOH, 100% EtOH and SafeClear. After drying, slides were mounted with mounting medium (Trevigen). For α v integrin ICC, Alexa Fluor 647-conjugated secondary antibody (Molecular Probes) was used. Slides were mounted with Prolong Gold Antifade with DAPI (Thermo Fisher Scientific). Imaging was performed using the Axioplan 2 microscope in the Icahn School of Medicine Microscopy Shared Resource Facility.

RNA extraction and RT-qPCR

TRI Reagent RT kit (MRC) was used to extract total RNA from cell lysates. RNA was cleaned with RNeasy Mini Elute Cleanup Kit (Qiagen). cDNA was generated from 1 mg total RNA using the Superscript First Strand and oligo dT (Invitrogen). Absolute Blue qPCR master mix (Thermo Fisher Scientific) was used to generate PCR product. Triplicate determinations were analyzed using the ABI 7900 sequence detection system. Annealing temperature was 55°C for all reactions. Primers used: β 5 (IDT): 5'-CTGTCCATGAAGGATGACTT-3', 5'-TGTCCACTCTGTCTGTGAGA-3'; α v (IDT): 5'-GTGGACAGTCTGCCGAGTAC-3', 5'-GAGCTCCACGAGAAGAAACA-3'; β 1 (IDT): 5'-TCAAAAGCCAGGACGCAACTC-3', TCCACTGATGTCCCGTTTCGAG-3'; GAPDH (Invitrogen): 5'-TTGATTTGGAGGGATCTCG-3', 5'-GAGTCAACGGATTGGTTCGT-3'; FN-EDA (IDT): 5'-TCCAAGCGGAGAGAG-3', 5'-GTGGGTGTGACC-TGA-3'; SMA (IDT): 5'-CATCTCGTTTCAAAGTCCAGAGC-3', 5'-TGAGCGTGGCTATTCCTCGT-3'; USP10 (IDT): 5'-GATCCTCTGAAACCGGAACA-3', 5'-AGAGTGCATCACCTCCTGCT-3'.

TGF β activity assay

TGF β activity was measured using cell lines constitutively expressing pGreenFire Lenti-Reporter (System Biosciences), a reporter for SMAD activation. This reporter was used to generate TGF β reporter cell lines with hTERT fibroblasts (hTERT-SMAD) and 293t cells (293t-SMAD). To assess TGF β activity with USP10 overexpression, 50K hTERT-SMAD cells

were co-cultured with 50K cells constitutively overexpressing USP10 (hTERT-USP10) or control cells, hTERT cells expressing empty vector (hTERT-vector cells) either or alone or hTERT-USP10 with 100 nM α v blocking compound CWHM12 or control compound CWHM96. After 24 h, cells were removed with trypsin, pelleted, re-suspended in luciferase reagent, placed in wells in triplicate, and assayed for luciferase expression with a Biotek plate reader. To assess TGF β activity when USP10 was silenced, USP10 and control siRNA were transiently transfected in 293t-SMAD cells and assayed as above.

Total TGF β assay

Total TGF β levels were quantified using the Quantikine ELISA kit (R&D Systems). USP10-overexpressing cells and control cells were plated in SSFM for 48 h. After 48 h, the cell culture supernatants were collected and centrifuged at 1000 rpm for 5 min prior to treatment with 1 N HCl for 10 min to activate latent TGF β . The supernatants were then neutralized by addition of 1.2 N NaOH/0.5 M HEPES. The activated USP10 and control cell supernatants were used in the ELISA. A TGF β standard curve in a range of 15.65 pg/ml to 1000 pg/ml was generated. After a 2 h incubation, wells were washed and incubated for 2 h with TGF β 1 Conjugate followed by detection reagent and reading at 450 nm wavelength (Biotek plate reader).

Statistical analysis

Numerical data are expressed as mean \pm s.d. of 3–5 independent experiments. Statistical significance for histological analysis of three groups (nonwounded, wounded plus control siRNA and wounded plus USP10 siRNA) was calculated by one-way ANOVA with Bonferroni's test. Statistical significance of all other numerical data was calculated with the Student's *t*-test.

Acknowledgements

Microscopy and image analysis was performed at the Microscopy CORE, histological slide preparation was performed at the Biorepository and Pathology CORE, and RNAseq was performed at the Genomics Core at the Icahn School of Medicine at Mount Sinai. We are grateful to Dr Liliana Ossowski for critical reading of the manuscript, Dr Zheng Wang for technical support and Dr Ravi Sachidanandam for assistance with RNAseq data processing.

Competing interests

The authors declare no competing or financial interests.

Author contributions

Conceptualization: S.R.G., A.M.B.; Methodology: S.R.G., L.W., A.M.B.; Validation: S.R.G., A.M.B.; Formal analysis: S.R.G., L.J.T., L.W., A.M.B.; Investigation: S.R.G., A.M.B.; Resources: A.M.B.; Data curation: S.R.G., L.J.T., L.W.; Writing - original draft: A.M.B.; Writing - review & editing: S.R.G., A.M.B.; Visualization: A.M.B.; Supervision: A.M.B.; Project administration: A.M.B.; Funding acquisition: A.M.B.

Funding

This work was supported by Research to Prevent Blindness and the Office for Extramural Research, National Institutes of Health (R01 EY024942 to A.M.B. and T32 GM 062754 to S.R.G.). Deposited in PMC for release after 12 months.

Supplementary information

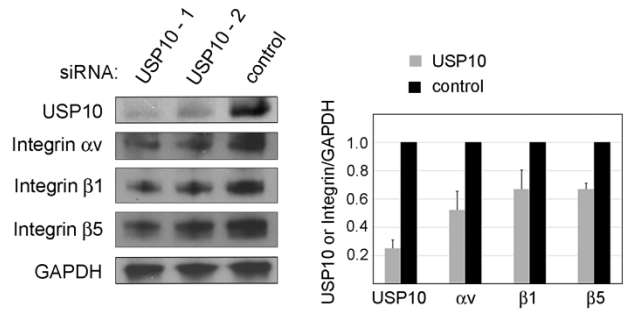
Supplementary information available online at <http://jcs.biologists.org/lookup/doi/10.1242/jcs.204628.supplemental>

References

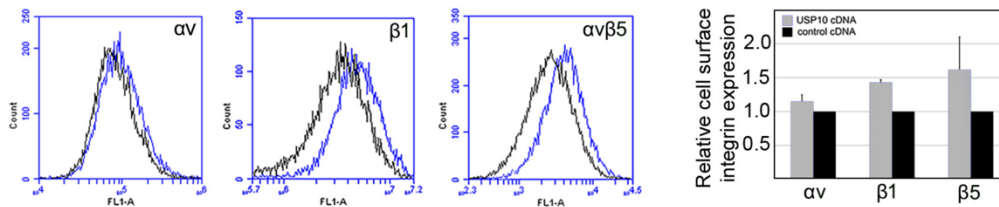
- Abdalla, M., Goc, A., Segar, L. and Somanath, P. R. (2013). Akt1 mediates alpha-smooth muscle actin expression and myofibroblast differentiation via myocardin and serum response factor. *J. Biol. Chem.* **288**, 33483-33493.
- Abe, M., Yokoyama, Y. and Ishikawa, O. (2012). A possible mechanism of basic fibroblast growth factor-promoted scarless wound healing: the induction of myofibroblast apoptosis. *Eur. J. Dermatol.* **22**, 46-53.
- Asano, Y., Ihn, H., Yamane, K., Jinnin, M., Mimura, Y. and Tamaki, K. (2005). Involvement of alphavbeta5 integrin-mediated activation of latent transforming growth factor beta1 in autocrine transforming growth factor beta signaling in systemic sclerosis fibroblasts. *Arthritis. Rheum.* **52**, 2897-2905.
- Asano, Y., Ihn, H., Jinnin, M., Mimura, Y. and Tamaki, K. (2006a). Involvement of alphavbeta5 integrin in the establishment of autocrine TGF-beta signaling in dermal fibroblasts derived from localized scleroderma. *J. Invest. Dermatol.* **126**, 1761-1769.

- Asano, Y., Ihn, H., Yamane, K., Jinnin, M. and Tamaki, K. (2006b). Increased expression of integrin alphavbeta5 induces the myofibroblastic differentiation of dermal fibroblasts. *Am. J. Pathol.* **168**, 499-510.
- Barbosa, F. L., Chaurasia, S. S., Cutler, A., Asosingh, K., Kaur, H., de Medeiros, F. W., Agrawal, V. and Wilson, S. E. (2010). Corneal myofibroblast generation from bone marrow-derived cells. *Exp. Eye Res.* **91**, 92-96.
- Becker, A., von Richter, O., Kovar, A., Scheible, H., van Lier, J. J. and John, A. (2015). Metabolism and disposition of the alphav-integrin ss3/ss5 receptor antagonist cilengtide, a cyclic polypeptide, in humans. *J. Clin. Pharmacol.* **55**, 815-824.
- Bernstein, A. M., Twining, S. S., Warejcka, D. J., Tall, E. and Masur, S. K. (2007). Urokinase receptor cleavage: a crucial step in fibroblast-to-myofibroblast differentiation. *Mol. Biol. Cell* **18**, 2716-2727.
- Bharadwaj, M., Strohmeier, N., Colo, G. P., Helenius, J., Beerenwinkel, N., Schiller, H. B., Fässler, R. and Müller, D. J. (2017). alphaV-class integrins exert dual roles on alpha5beta1 integrins to strengthen adhesion to fibronectin. *Nat. Commun.* **8**, 14348.
- Bomberger, J. M., Barnaby, R. L. and Stanton, B. A. (2009). The deubiquitinating enzyme USP10 regulates the post-endocytic sorting of cystic fibrosis transmembrane conductance regulator in airway epithelial cells. *J. Biol. Chem.* **284**, 18778-18789.
- Bomberger, J. M., Barnaby, R. L. and Stanton, B. A. (2010). The deubiquitinating enzyme USP10 regulates the endocytic recycling of CFTR in airway epithelial cells. *Channels (Austin)* **4**, 150-154.
- Boukroun, S., Ruffieux-Daidie, D., Vitagliano, J.-J., Poirot, O., Charles, R.-P., Lagnaz, D., Firsov, D., Kellenberger, S. and Staub, O. (2008). Vasopressin-inducible ubiquitin-specific protease 10 increases ENaC cell surface expression by deubiquitylating and stabilizing sorting nexin 3. *Am. J. Physiol. Renal. Physiol.* **295**, F889-F900.
- Chandler, H. L., Colitz, C. M. H., Lu, P., Saville, W. J. A. and Kusewitt, D. F. (2007). The role of the slug transcription factor in cell migration during corneal re-epithelialization in the dog. *Exp. Eye Res.* **84**, 400-411.
- Chang, Y., Lau, W. L., Jo, H., Tsujino, K., Gewin, L., Reed, N. I., Atakilit, A., Nunes, A. C., DeGrado, W. F. and Sheppard, D. (2017). Pharmacologic blockade of alphavbeta1 integrin ameliorates renal failure and fibrosis in vivo. *J. Am. Soc. Nephrol.* **28**, 1998-2005.
- Conroy, K. P., Kitto, L. J. and Henderson, N. C. (2016). alphav integrins: key regulators of tissue fibrosis. *Cell Tissue Res.* **365**, 511-519.
- Crawford, L. J., Walker, B. and Irvine, A. E. (2011). Proteasome inhibitors in cancer therapy. *J. Cell Commun. Signal.* **5**, 101-110.
- Defilles, C., Lissitzky, J.-C., Montero, M.-P., André, F., Prévot, C., Delamarre, E., Marrakchi, N., Luis, J. and Rigot, V. (2009). alphavbeta5/beta6 integrin suppression leads to a stimulation of alpha2beta1 dependent cell migration resistant to PI3K/Akt inhibition. *Exp. Cell Res.* **315**, 1840-1849.
- Deng, H. X., Chen, W., Hong, S. T., Boycott, K. M., Gorrie, G. H., Siddique, N., Yang, Y., Fecto, F., Shi, Y., Zhai, H. et al. (2011). Mutations in UBQLN2 cause dominant X-linked juvenile and adult-onset ALS and ALS/dementia. *Nature* **477**, 211-215.
- do Carmo Costa, M., Bajanca, F., Rodrigues, A. J., Tome, R. J., Corthals, G., Macedo-Ribeiro, S., Paulson, H. L., Logarinho, E. and Maciel, P. (2010). Ataxin-3 plays a role in mouse myogenic differentiation through regulation of integrin subunit levels. *PLoS ONE* **5**, e11728.
- Duperret, E. K., Natale, C. A., Monteleon, C., Dahal, A. and Ridky, T. W. (2016). The integrin alphav-TGFbeta signaling axis is necessary for epidermal proliferation during cutaneous wound healing. *Cell Cycle*, 1-10. **15**, 2077-2086.
- Dupont, S., Mamidi, A., Cordenonsi, M., Montagner, M., Zacchigna, L., Adorno, M., Martello, G., Stinchfield, M. J., Soligo, S., Morsut, L. et al. (2009). FAM/USP9x, a deubiquitinating enzyme essential for TGFbeta signaling, controls Smad4 monoubiquitination. *Cell* **136**, 123-135.
- Farshi, P., Deshmukh, R. R., Nwankwo, J. O., Arkwright, R. T., Cvek, B., Liu, J. and Dou, Q. P. (2015). Deubiquitinases (DUBs) and DUB inhibitors: a patent review. *Expert Opin. Ther. Pat.* **25**, 1191-1208.
- Goffin, J. M., Pittet, P., Csucs, G., Lussi, J. W., Meister, J.-J. and Hinz, B. (2006). Focal adhesion size controls tension-dependent recruitment of alpha-smooth muscle actin to stress fibers. *J. Cell Biol.* **172**, 259-268.
- He, W. and Dai, C. (2015). Key fibrogenic signaling. *Curr. Pathobiol. Rep.* **3**, 183-192.
- Henderson, N. C. and Sheppard, D. (2013). Integrin-mediated regulation of TGFbeta in fibrosis. *Biochim. Biophys. Acta* **1832**, 891-896.
- Henderson, N. C., Arnold, T. D., Katamura, Y., Giacomini, M. M., Rodriguez, J. D., McCarty, J. H., Pellicoro, A., Raschperger, E., Betsholtz, C., Ruminski, P. G. et al. (2013). Targeting of alphav integrin identifies a core molecular pathway that regulates fibrosis in several organs. *Nat. Med.* **19**, 1617-1624.
- Hinz, B. (2015). The extracellular matrix and transforming growth factor-beta1: tale of a strained relationship. *Matrix Biol.* **47**, 54-65.
- Hinz, B. (2007). Formation and function of the myofibroblast during tissue repair. *J. Invest. Dermatol.* **127**, 526-537.
- Hinz, B. and Gabbiani, G. (2010). Fibrosis: recent advances in myofibroblast biology and new therapeutic perspectives. *F1000 Biol. Rep.* **2**, 78.
- Horowitz, J. C., Rogers, D. S., Sharma, V., Vittal, R., White, E. S., Cui, Z. and Thannickal, V. J. (2007). Combinatorial activation of FAK and AKT by transforming growth factor-beta1 confers an anoikis-resistant phenotype to myofibroblasts. *Cell. Signal.* **19**, 761-771.
- Hsia, H. C., Nair, M. R. and Corbett, S. A. (2014). The fate of internalized alpha5 integrin is regulated by matrix-capable fibronectin. *J. Surg. Res.* **191**, 268-279.
- Hussain, S., Zhang, Y. and Galardy, P. (2009). DUBs and cancer: the role of deubiquitinating enzymes as oncogenes, non-oncogenes and tumor suppressors. *Cell Cycle* **8**, 1688-1697.
- Imamura, R., Isaka, Y., Sandoval, R. M., Ori, A., Adamsky, S., Feinstein, E., Molitoris, B. A. and Takahara, S. (2010). Intravital two-photon microscopy assessment of renal protection efficacy of siRNA for p53 in experimental rat kidney transplantation models. *Cell Transplant.* **19**, 1659-1670.
- Janin-Manificat, H., Rovere, M. R., Galiacy, S. D., Malecaze, F., Hulmes, D. J., Moali, C. and Damour, O. (2012). Development of ex vivo organ culture models to mimic human corneal scarring. *Mol. Vis.* **18**, 2896-2908.
- Jester, J. V., Huang, J., Petroll, W. M. and Cavanagh, H. D. (2002). TGFbeta induced myofibroblast differentiation of rabbit keratocytes requires synergistic TGFbeta, PDGF and integrin signaling. *Exp. Eye Res.* **75**, 645-657.
- Jester, J. V., Huang, J., Fisher, S., Spiekerman, J., Chang, J. H., Wright, W. E. and Shay, J. W. (2003). Myofibroblast differentiation of normal human keratocytes and hTERT, extended-life human corneal fibroblasts. *Invest. Ophthalmol. Vis. Sci.* **44**, 1850-1858.
- Kanno, Y., Kaneiwa, A., Minamida, M., Kanno, M., Tomogane, K., Takeuchi, K., Okada, K., Ueshima, S., Matsuo, O. and Matsuno, H. (2008). The absence of uPAR is associated with the progression of dermal fibrosis. *J. Invest. Dermatol.* **128**, 2792-2797.
- Kapp, T. G., Rechenmacher, F., Sobahi, T. R. and Kessler, H. (2013). Integrin modulators: a patent review. *Expert Opin. Ther. Pat.* **23**, 1273-1295.
- Kim, S. J., Angel, P., Lafyatis, R., Hattori, K., Kim, K. Y., Sporn, M. B., Karin, M. and Roberts, A. B. (1990). Autoinduction of transforming growth factor beta 1 is mediated by the AP-1 complex. *Mol. Cell Biol.* **10**, 1492-1497.
- Kim, J. T., Lee, E. H., Chung, K. H., Kang, I. C., Lee, D. H. and Joo, C. K. (2004). Transdifferentiation of cultured bovine lens epithelial cells into myofibroblast-like cells by serum modulation. *Yonsei Med. J.* **45**, 380-391.
- Klingberg, F., Chow, M. L., Koehler, A., Boo, S., Buscemi, L., Quinn, T. M., Costell, M., Alman, B. A., Genot, E. and Hinz, B. (2014). Prestress in the extracellular matrix sensitizes latent TGF-beta1 for activation. *J. Cell Biol.* **207**, 283-297.
- Leask, A. (2013). Integrin beta1: a mechanosignaling sensor essential for connective tissue deposition by fibroblasts. *Adv. Wound Care (New Rochelle)* **2**, 160-166.
- Liu, K. Y., Timmons, S., Lin, Y. Z. and Hawiger, J. (1996). Identification of a functionally important sequence in the cytoplasmic tail of integrin beta 3 by using cell-permeable peptide analogs. *Proc. Natl. Acad. Sci. USA* **93**, 11819-11824.
- Lobert, V. H. and Stenmark, H. (2010). Ubiquitination of alpha-integrin cytoplasmic tails. *Commun. Integr. Biol.* **3**, 583-585.
- Lobert, V. H., Brech, A., Pedersen, N. M., Wesche, J., Oppelt, A., Malerød, L. and Stenmark, H. (2010). Ubiquitination of alpha 5 beta 1 integrin controls fibroblast migration through lysosomal degradation of fibronectin-integrin complexes. *Dev. Cell* **19**, 148-159.
- Loch, C. M. and Strickler, J. E. (2012). A microarray of ubiquitylated proteins for profiling deubiquitylase activity reveals the critical roles of both chain and substrate. *Biochim. Biophys. Acta* **1823**, 2069-2078.
- Mamuya, F. A., Wang, Y., Roop, V. H., Scheiblin, D. A., Zajac, J. C. and Duncan, M. K. (2014). The roles of alphaV integrins in lens EMT and posterior capsular opacification. *J. Cell. Mol. Med.* **18**, 656-670.
- Manetti, M., Rosa, I., Milia, A. F., Guiducci, S., Carmeliet, P., Ibba-Manneschi, L. and Matucci-Cerinic, M. (2014). Inactivation of urokinase-type plasminogen activator receptor (uPAR) gene induces dermal and pulmonary fibrosis and peripheral microvasculopathy in mice: a new model of experimental scleroderma? *Ann. Rheum. Dis.* **73**, 1700-1709.
- Manetti, M., Rosa, I., Fazi, M., Guiducci, S., Carmeliet, P., Ibba-Manneschi, L. and Matucci-Cerinic, M. (2016). Systemic sclerosis-like histopathological features in the myocardium of uPAR-deficient mice. *Ann. Rheum. Dis.* **75**, 474-478.
- Masur, S. K., Cheung, J. K. and Antohi, S. (1993). Identification of integrins in cultured corneal fibroblasts and in isolated keratocytes. *Invest. Ophthalmol. Vis. Sci.* **34**, 2690-2698.
- Miller, C. G., Pozzi, A., Zent, R. and Schwarzbauer, J. E. (2014). Effects of high glucose on integrin activity and fibronectin matrix assembly by mesangial cells. *Mol. Biol. Cell* **25**, 2342-2350.
- Molitoris, B. A., Dagher, P. C., Sandoval, R. M., Campos, S. B., Ashush, H., Fridman, E., Brafman, A., Faerman, A., Atkinson, S. J., Thompson, J. D. et al. (2009). siRNA targeted to p53 attenuates ischemic and cisplatin-induced acute kidney injury. *J. Am. Soc. Nephrol.* **20**, 1754-1764.
- Muro, A. F., Moretti, F. A., Moore, B. B., Yan, M., Atrasz, R. G., Wilke, C. A., Flaherty, K. R., Martinez, F. J., Tsui, J. L., Sheppard, D. et al. (2008). An essential role for fibronectin extra type III domain A in pulmonary fibrosis. *Am. J. Respir. Crit. Care Med.* **177**, 638-645.

- Pan, L., Chen, Z., Wang, L., Chen, C., Li, D., Wan, H., Li, B. and Shi, G. (2014). Deubiquitination and stabilization of T-bet by USP10. *Biochem. Biophys. Res. Commun.* **449**, 289-294.
- Parapuram, S. K. and Hodge, W. (2014). The integrin needle in the stromal haystack: emerging role in corneal physiology and pathology. *J. Cell Commun. Signal.* **8**, 113-124.
- Pasqualini, R. and Hemler, M. E. (1994). Contrasting roles for integrin beta 1 and beta 5 cytoplasmic domains in subcellular localization, cell proliferation, and cell migration. *J. Cell Biol.* **125**, 447-460.
- Reed, N. I., Jo, H., Chen, C., Tsujino, K., Arnold, T. D., DeGrado, W. F. and Sheppard, D. (2015). The alphavbeta1 integrin plays a critical in vivo role in tissue fibrosis. *Sci. Transl. Med.* **7**, 288ra79.
- Reimand, J., Arak, T., Adler, P., Kolberg, L., Reisberg, S., Peterson, H. and Vilo, J. (2016). g:Profiler—a web server for functional interpretation of gene lists (2016 update). *Nucleic Acids Res.* **44**, W83-W89.
- Riederer, B. M., Leuba, G., Vernay, A. and Riederer, I. M. (2011). The role of the ubiquitin proteasome system in Alzheimer's disease. *Exp. Biol. Med. (Maywood)* **236**, 268-276.
- Sarrazay, V., Koehler, A., Chow, M. L., Zimina, E., Li, C. X., Kato, H., Caldarone, C. A. and Hinz, B. (2014). Integrins alphavbeta5 and alphavbeta3 promote latent TGF-beta1 activation by human cardiac fibroblast contraction. *Cardiovasc. Res.* **102**, 407-417.
- Sechler, J. L., Takada, Y. and Schwarzbauer, J. E. (1996). Altered rate of fibronectin matrix assembly by deletion of the first type III repeats. *J. Cell Biol.* **134**, 573-583.
- Scotton, C. J., Krupiczkoj, M. A., Konigshoff, M., Mercer, P. F., Lee, Y. C., Kaminski, N., Morser, J., Post, J. M., Maher, T. M., Nicholson, A. G. et al. (2009). Increased local expression of coagulation factor X contributes to the fibrotic response in human and murine lung injury. *J. Clin. Investig.* **119**, 2550-2563.
- Shinde, A. V., Kelsh, R., Peters, J. H., Sekiguchi, K., Van De Water, L. and McKeown-Longo, P. J. (2014). The alpha4beta1 integrin and the EDA domain of fibronectin regulate a profibrotic phenotype in dermal fibroblasts. *Matrix Biol.* **41**, 26-35.
- Sigismund, S. and Polo, S. (2016). Strategies to detect endogenous ubiquitination of a target mammalian protein. *Methods Mol. Biol.* **1449**, 143-151.
- Sowa, M. E., Bennett, E. J., Gyji, S. P. and Harper, J. W. (2009). Defining the human deubiquitinating enzyme interaction landscape. *Cell* **138**, 389-403.
- Stepp, M. A., Zieske, J. D., Trinkaus-Randall, V., Kyne, B. M., Pal-Ghosh, S., Tadvalkar, G. and Pajoohesh-Ganji, A. (2014). Wounding the cornea to learn how it heals. *Exp. Eye Res.* **121**, 178-193.
- Stuelten, C. H., Kamaraju, A. K., Wakefield, L. M. and Roberts, A. B. (2007). Lentiviral reporter constructs for fluorescence tracking of the temporospatial pattern of Smad3 signaling. *BioTechniques* **43**, 289-290, 292, 294.
- Taherian, A., Li, X., Liu, Y. and Haas, T. A. (2011). Differences in integrin expression and signaling within human breast cancer cells. *BMC Cancer* **11**, 293.
- Takahashi, M., Higuchi, M., Matsuki, H., Yoshita, M., Ohsawa, T., Oie, M. and Fujii, M. (2012). Stress granules inhibit apoptosis by reducing reactive oxygen species production. *Mol. Cell. Biol.* **33**, 815-829.
- Taliana, L., Benezra, M., Greenberg, R. S., Masur, S. K. and Bernstein, A. M. (2005). ZO-1: lamellipodial localization in a corneal fibroblast wound model. *Invest. Ophthalmol. Vis. Sci.* **46**, 96-103.
- Thompson, J. D., Kornbrust, D. J., Foy, J. W., Solano, E. C., Schneider, D. J., Feinstein, E., Molitoris, B. A. and Erlich, S. (2012). Toxicological and pharmacokinetic properties of chemically modified siRNAs targeting p53 RNA following intravenous administration. *Nucleic Acid Ther.* **22**, 255-264.
- Tomasek, J. J., McRae, J., Owens, G. K. and Haaksma, C. J. (2005). Regulation of alpha-smooth muscle actin expression in granulation tissue myofibroblasts is dependent on the intronic CARg element and the transforming growth factor-beta1 control element. *Am. J. Pathol.* **166**, 1343-1351.
- Ulmasov, B., Neuschwander-Tetri, B. A., Lai, J., Monastyrskiy, V., Bhat, T., Yates, M. P., Oliva, J., Prinsen, M. J., Ruminski, P. G. and Griggs, D. W. (2016). Inhibitors of Arg-Gly-Asp-binding integrins reduce development of pancreatic fibrosis in mice. *Cell Mol. Gastroenterol. Hepatol.* **2**, 499-518.
- Van De Water, L., Varney, S. and Tomasek, J. J. (2013). Mechanoregulation of the myofibroblast in wound contraction, scarring, and fibrosis: opportunities for new therapeutic intervention. *Adv. Wound Care (New Rochelle)* **2**, 122-141.
- Wang, L., Pedroja, B. S., Meyers, E. E., Garcia, A. L., Twining, S. S. and Bernstein, A. M. (2012). Degradation of internalized alphavbeta5 integrin is controlled by uPAR bound uPA: effect on beta1 integrin activity and alpha-SMA stress fiber assembly. *PLoS ONE* **7**, e33915.
- Whitcher, J. P., Srinivasan, M. and Upadhyay, M. P. (2001). Corneal blindness: a global perspective. *Bull. World Health Organ.* **79**, 214-221.
- White, E. S. and Muro, A. F. (2011). Fibronectin splice variants: understanding their multiple roles in health and disease using engineered mouse models. *IUBMB Life* **63**, 538-546.
- Wierzbicka-Patynowski, I. and Schwarzbauer, J. E. (2003). The ins and outs of fibronectin matrix assembly. *J. Cell Sci.* **116**, 3269-3276.
- Wilson, S. E., Chaurasia, S. S. and Medeiros, F. W. (2007). Apoptosis in the initiation, modulation and termination of the corneal wound healing response. *Exp. Eye Res.* **85**, 305-311.
- Wilson, C. L., Murphy, L. B., Leslie, J., Kendrick, S., French, J., Fox, C. R., Sheerin, N. S., Fisher, A., Robinson, J. H., Tiniakos, D. G. et al. (2015). Ubiquitin C-terminal hydrolase 1: a novel functional marker for liver myofibroblasts and a therapeutic target in chronic liver disease. *J. Hepatol.* **63**, 1421-1428.
- Wipff, P.-J., Rifkin, D. B., Meister, J.-J. and Hinz, B. (2007). Myofibroblast contraction activates latent TGF-beta1 from the extracellular matrix. *J. Cell Biol.* **179**, 1311-1323.
- Xia, H., Nho, R. S., Kahm, J., Kleidon, J. and Henke, C. A. (2004). Focal adhesion kinase is upstream of phosphatidylinositol 3-kinase/Akt in regulating fibroblast survival in response to contraction of type I collagen matrices via a beta 1 integrin viability signaling pathway. *J. Biol. Chem.* **279**, 33024-33034.
- Yang, Y., Wang, Z., Yang, H., Wang, L., Gillespie, S. R., Wolosin, J. M., Bernstein, A. M. and Reinach, P. S. (2013). TRPV1 potentiates TGFbeta1-induced of corneal myofibroblast development through an oxidative stress-mediated p38-SMAD2 signaling loop. *PLoS ONE* **8**, e77300.
- Yang, N., Yu, F., Shao, G., Fu, Y. and Kong, W. (2016). The E3 ubiquitin ligase c-Cbl mediates integrin beta1 ubiquitination during dilated cardiomyopathy. *Biochem. Biophys. Res. Commun.* **479**, 728-735.
- Yuan, J., Luo, K., Zhang, L., Cheville, J. C. and Lou, Z. (2010). USP10 regulates p53 localization and stability by deubiquitinating p53. *Cell* **140**, 384-396.
- Zhou, Y., Hagood, J. S., Lu, B., Merryman, W. D. and Murphy-Ullrich, J. E. (2010). Thy-1-integrin alphav beta5 interactions inhibit lung fibroblast contraction-induced latent transforming growth factor-beta1 activation and myofibroblast differentiation. *J. Biol. Chem.* **285**, 22382-22393.
- Zieske, J. D., Guimarães, S. R. and Hutcheon, A. E. K. (2001). Kinetics of keratocyte proliferation in response to epithelial debridement. *Exp. Eye Res.* **72**, 33-39.



Supplemental Fig 1. HCFs were transfected with two unique USP10 siRNAs (Dharmacon), or control siRNA. After 48 hours, cells were lysed and Western blotted for USP10, integrins αv , $\beta 1$, $\beta 5$, and GAPDH. The results of the knockdown using the two USP10 siRNAs were averaged. USP10 was decreased (75.1% +/- 6.0%), αv (47.8% +/- 13.0%), $\beta 1$ (33.2% +/- 13.4%), and $\beta 5$ (33.2% +/- 4.2%). Representative blot is shown. N=3.



Supplemental Fig 2. Flow cytometry analysis of cell-surface integrin levels after USP10 overexpression. Flow cytometry for cell-surface integrin αv , $\beta 1$, and $\alpha v\beta 5$, (representative experiment shown), average increases- αv (1.15 +/- 0.09), $\beta 1$ (1.43 +/- 0.04) 1.62 fold +/- 0.48) N=3.

$\beta 1$	HDRREFAKFEKEKMNAKWDGTGENPIYKSAVTTVVNPKYEGK
$\beta 3$	HDRKEFAKFEEERARAKWDTANNPLYKEATSTFTNITYRGT
$\beta 5$	HDRREFAKFQSERSRARYEMASNPLYRKPISTHTVDFTFNKFNKSYNGTVD

Supplemental Fig 3. The cytoplasmic tails of integrins $\beta 1$, $\beta 3$, and $\beta 5$. The lysines, which are potential sites for ubiquitination, are highlighted in blue.